Author/s:
Nguyen, THO;Foo, IJH;Purcell, RA;Tan, HX;Deliyannis, G;Zhang, W;Carolan, L;Hadiprodjo, AJ;Huang, HH;Allen, LF;Hagen, RR;Aurelia, LC;McQuilten, HA;Rowntree, LC;Kedzierski, L;Wilks, SH;McKay, MR;Tannock, GA;Kent, SJ;Laurie, K;Fox, A;Rockman, S;Brown, LE;Chung, AW;Wheatley, AK;Kedzierska, K

Title:
Historic 1994 influenza vaccine cohorts define breadth of antibody and B cell responses toward future influenza A and B viruses

Date:
2026

Citation:
Nguyen, T. H. O., Foo, I. J. H., Purcell, R. A., Tan, H. X., Deliyannis, G., Zhang, W., Carolan, L., Hadiprodjo, A. J., Huang, H. H., Allen, L. F., Hagen, R. R., Aurelia, L. C., McQuilten, H. A., Rowntree, L. C., Kedzierski, L., Wilks, S. H., McKay, M. R., Tannock, G. A., Kent, S. J. ,... Kedzierska, K. (2026). Historic 1994 influenza vaccine cohorts define breadth of antibody and B cell responses toward future influenza A and B viruses. Science Translational Medicine, 18 (843), https://doi.org/10.1126/scitranslmed.aea8621.

Historic 1994 influenza vaccine cohorts define breadth of antibody and B cell responses towards future influenza A and B viruses

Authors: Thi H. O. Nguyen[1]†, Isabelle J. H. Foo[1]†, Ruth A. Purcell[1]†, Hyon-Xhi Tan[1]†, Georgia Deliyannis[1], Wuji Zhang[1], Louise Carolan[2], A. Jessica Hadiprodjo[2], Howard H. Huang[1], Lilith F. Allen[1], Ruth R. Hagen[1], L. Carissa Aurelia[1], Hayley A. McQuilten[1], Louise C. Rowntree[1], Lukasz Kedzierski[1], Samuel H. Wilks[3,4], Matthew R. McKay[1,3,4], Gregory A. Tannock[5], Stephen J. Kent[1,6], Karen Laurie[7], Annette Fox[2,8], Steven Rockman[1,7], Lorena E. Brown[1,9], Amy W. Chung[1]‡, Adam K. Wheatley[1]‡ and Katherine Kedzierska[1,9]*‡

Affiliations:

[1]Department of Microbiology and Immunology, University of Melbourne, at the Peter Doherty Institute for Infection and Immunity, Melbourne, Victoria 3000, Australia.

[2]WHO Collaborating Centre for Reference and Research on Influenza, Royal Melbourne Hospital, at the Peter Doherty Institute for Infection and Immunity, Melbourne, Victoria 3000, Australia.

[3]Department of Electrical and Electronic Engineering, University of Melbourne, Melbourne, Victoria 3010, Australia.

[4]Victorian Infectious Diseases Reference Laboratory, at the Peter Doherty Institute for Infection and Immunity, Melbourne, Victoria 3000, Australia.

[5]Burnet Institute, Melbourne, Victoria 3004, Australia.

[6]Melbourne Sexual Health Centre and Department of Infectious Diseases, Alfred Health, Central Clinical School, Monash University, Melbourne, Victoria 3004, Australia.

[7]CSL Seqirus Ltd, Parkville, Victoria 3052, Australia.

[8]Department of Infectious Diseases, University of Melbourne, at the Peter Doherty Institute for Infection and Immunity, Melbourne, Victoria 3000, Australia.

[9]Institute for Vaccine Research and Development, Hokkaido University, Sapporo, Hokkaido 060-0808, Japan.

*e-mail: kkedz@unimelb.edu.au

†These authors contributed equally to this work.

‡These authors jointly supervised this work.

One Sentence Summary: B cell responses that bound to future H1N1 and influenza B virus strains, but not H3N2 strains, were elicited in adults by the 1994 influenza vaccine.

ABSTRACT

Vaccination is the best way to combat annual influenza epidemics, yet the breadth of vaccine-induced humoral immunity towards decades of future differentially evolving influenza A (IAV) and B (IBV) viruses is unclear. Using historic 1994 influenza vaccination cohorts of young and older adults, we defined antibody responses elicited by 1994 vaccination against future influenza strains spanning three decades of differentially evolving IAV and IBV strains. The quality of antibody responses and vaccine-induced and cross-reactive B cell memory responses were also investigated. Vaccination increased antibody titers against all 1994 vaccine components in younger and older adults. Antibodies that bind to future H1N1 strains were also detected across younger and older adults, including non-neutralizing hemagglutinin (HA) stem antibody responses. Prominent boosting against earlier B/Yamagata/16/1988 and future Yamagata-lineage strains were also observed, but antibody responses towards future rapidly evolving H3N2 strains were minimal. Systems serology revealed divergent antibody signatures between younger and older adults against future antigens. However, post-vaccination responses were of high-quality in both age groups. 1994 vaccination-induced cross-reactive HA-specific memory B cells bound to vaccine and future H1 and IBV strains, but exhibited minimal responses against H3. Group 1 cross-reactive H1/H5 stalk-specific responses also contributed to the overall H1 future response, whereas cross-reactive H3/H7 stalk-specific B cells were not detected. Our study provides insights into the breadth of vaccine-induced humoral immunity towards future influenza viruses over 30 years of influenza virus evolution, including newly emerging pandemic strains, and highlights the unmet need to optimize future vaccines strategies, especially for H3N2.

INTRODUCTION

Over the past 30 years, seasonal inactivated influenza vaccines (IIV) continue to be the most effective strategy to prevent influenza virus infection. The trivalent IIV covers two influenza A virus (IAV) strains (H1N1 and H3N2) and one influenza B virus (IBV) strain (Victoria or Yamagata lineage). IIVs, traditionally being egg-based vaccines, have since progressed to include quadrivalent vaccines including both IBV lineages, cell-based vaccines for people aged ≥ 6 months, high dose vaccines for ≥ 60 years, and adjuvanted vaccines for ≥ 65 years. People aged ≥ 65 years respond poorly to IIV (*1, 2*) and are more susceptible to influenza illness requiring hospitalization and death, accounting for 50–70% and 70–85% of cases, respectively (*3*). Adjuvanted vaccines are recommended for older adults in preference to the standard dose since they can boost more potent B cell responses in this older population (*4, 5*). Due to the rapid evolution of H3N2, the H3N2 vaccine strain is often mismatched with the circulating strains (*6*). Therefore, vaccine efficacy against H3N2 strains is lowest compared with the slower evolving H1N1 and IBV strains (*6, 7*), with older adults being most affected (*2, 8*).

Antibody responses are typically measured serologically using a surrogate hemagglutinin (HA) inhibition (HAI) assay or microneutralization assay detecting HA-specific antibodies. B cell responses include generation of plasmablasts and HA-specific memory B cells, which positively correlate with increases in HAI antibody titers following IIV vaccination (*9*). Studies demonstrated that pre-existing immunity (i.e. prior exposures to influenza virus infections or vaccinations) and age-related effects can impact the magnitude and cross-reactive potential of the antibody and B cell response to seasonal influenza vaccination (*8, 10-14*). However, the breadth of vaccine-induced humoral immunity towards decades of future influenza A and B viruses in both adults and older adults is less defined.

Using historic 1994 influenza vaccination cohorts of younger and older adults, our goal was to define pre-vaccination antibody reactivity, and antibody responses elicited by 1994 influenza vaccination against future influenza virus strains spanning three decades of differentially evolving influenza subtypes (H1N1, H3N2 and IBV), including newly emerging pandemic strains. We also aimed to investigate the quality of antibody responses by defining antibody isotype, subclass, and effector function, as well as vaccine-boosted and cross-reactive B cell memory responses using contemporary methods such as systems serology and fluorescently-labelled recombinant HA-probes.

RESULTS

1994 IIV study cohort included younger and older adults

Our 1994 IIV cohort included 89 younger adults and 68 older adults vaccinated in April 1994 with the trivalent IIV Fluvax (Fig. 1A). The vaccine was derived from H1N1 A/Texas/36/1991, H3N2 A/Beijing/32/1992, and IBV Yamagata B/Panama/45/1990 reference strains. Blood samples were collected at baseline and approximately 28 days (d) following vaccination for plasma and peripheral blood mononuclear cells (PBMCs), then cryopreserved for 30 years. Subsets of samples were selected for HAI landscape, systems serology, and memory B cell responses. The full cohort had young adults at a median age of 19 years (range 18-53) and 46% female, whereas older adults had a median age of 69 years (range 60-75) and were 49% female (Fig. 1, B and C). Young adults were predominantly born in the 1970s (85% of young cohort) when IBV diverged into Yamagata and Victoria lineages (Fig. 1D). Older adults were mainly born in the 1920s (88% of older cohort) and were exposed to H1N1 from the 1918-1919 H1N1 prototypical pandemic virus until the late 1960s, when H2N2 emerged. One 75-year-old female was born during the 1918-1919 H1N1 pandemic, which spread globally and killed > 40 million people (*15*). The 1918 H1N1 pandemic virus was antigenically similar to the most recent 2009 H1N1 influenza pandemic virus that our cohort was not exposed to (*16*).

Antibody responses towards the 1994 IIV are increased in both young and older adults after vaccination

To evaluate antibody responses towards the 1994 vaccine strains, HAI assays were performed on a subset of 28 young adults and 28 older adults. A HAI antibody titer of 40 has been found to represent 50% protection (*17*). Young and older adults had increased HAI antibody titers following vaccination to all three strains ($P < 0.01$) (Fig. 1E). However, older adults had 1.7-2.6-fold higher baseline HAI titers across all vaccine strains ($P < 0.05$), and 3.0-3.1-fold higher d28 titers for H3N2 and IBV strains ($P < 0.01$), compared with younger adults. We found no significant differences in seroconversion rates between older adults and younger adults across all strains (Fig. 1F), where seroconversion describes a $\geq$ 4-fold increase in antibody titers from baseline levels. To determine the presence of HA stem-specific antibody responses, enzyme-linked immunosorbent assays (ELISAs) were performed using H1 and H3 stem antigens (Fig. 1G). We found increases in H1 stem antibodies in older adults ($P < 0.0001$) following 1994 IIV vaccination, with older adults already having high baseline levels of H1 stem antibodies ($P < 0.0001$), as well as following IIV ($P < 0.0001$). H3 stem responses were also increased in older adults ($P = 0.0095$), but not for younger adults.

Vaccine-induced antibody responses were generated against future H1N1 and IBV influenza virus strains

Previous studies have investigated how influenza vaccine antibody responses could back-boost previously circulating strains for H3N2 (*13*). In our study, we assessed future-boosting on the same subset of individuals (28 young and 28 older adults), measuring the 1994 vaccine-induced and boosted antibody responses towards future H1N1, H3N2, B/Yam and B/Vic influenza viruses included in the influenza vaccine over the past 3 decades (table S1), including the A/California/7/2009 H1N1 pandemic strain (Fig. 2A).

We observed modest increases in HAI titers towards 3 future H1N1 strains (A/Beijing/262/1995, A/Solomon Islands/3/2006 and A/California/7/2009) in both younger and older adults following IIV (Fig. 2, B and C). Seroconversion to these three future H1N1 strains ranged between 17.9-28.6% for younger adults and 14.3-28.6% for older adults (fig. S1). Antibody responses towards A/New Caledonia/20/1999 and A/Michigan/45/2015 were also observed for older adults, with A/Michigan/45/2015 being closely related to the 2009 pandemic strain (Fig. 2A). Compared with younger adults, older adults had higher baseline antibody titers towards A/New Caledonia/20/1999, pandemic A/California/7/2009 and pandemic-like A/Michigan/45/2015 strains ($P < 0.01$) which increased following IIV ($P < 0.05$) (Fig. 2C), suggesting more cross-reactive antibody responses to future strains including pandemic-like strains in older adults, although seroconversion rates for these strains were similar between the two age groups (fig. S1). Three older individuals (aged 69, 71, and 75) were seropositive for A/California/7/2009 and one 70-year-old was seropositive for A/Michigan/45/2015 at baseline (HAI = 40-80) (Fig. 2B), potentially having been exposed to the earlier 1918 pandemic strain, but only the eldest participant seroconverted against the pandemic strain following IIV. Although none of the younger adults were seropositive for A/California/7/2009 or A/Michigan/45/2015 at baseline (HAI < 40), three individuals did respond to either strain following IIV. In contrast, antibody responses towards future H3N2 strains were minimal (Fig. 2D), reflecting rapid evolution of H3N2. Only vaccine-directed responses against the earlier A/Port Chalmers/1/1973 strain were observed in older adults (Fig. 2E). Seroconversion to future H3N2 strains was also very low, ranging between 0.0-10.7% for younger adults and 3.6-14.3% for older adults (fig. S1).

Antibody responses were boosted against the earlier B/Yamagata/16/1988 and future B/Florida/4/2006 and B/Massachusetts/2/2012 Yamagata-lineage strains in both younger and older adults following vaccination (Fig. 2, F and G), with older adults having higher baseline and d28 antibody levels compared with younger adults ($P < 0.001$). Older adults also had

higher proportions of seroconverters towards B/Yamagata/16/1988 and B/Florida/4/2006 (43% and 64.7%, respectively) compared with younger adults (28.6% and 17.9%, respectively; $P < 0.05$) (fig. S1). Older adults also showed responses to future Yamagata-lineage B/Wisconsin/1/2010 as well as to previously circulating B/Victoria/02/1987 which was not evident for younger adults. Instead, boosting in younger adults was towards the future Victoria-lineage B/Malaysia/2506/2004 (Fig. 2G), with 21.4% seroconversion compared with 3.6% in older adults (fig. S1). Individuals who responded strongly to the B/Panama/45/1990 vaccine strain, especially younger adults, could respond to multiple future IBV strains from both lineages.

To support our HAI antibody findings towards future strains, we further performed microneutralization assay to quantify virus neutralizing antibodies for the vaccine strain and future strains for H1N1 and IBV. Microneutralization assays for the H3N2 vaccine and future strain were not performed, as we did not observe future boosting of H3N2 strains. We found an increase in neutralizing antibodies against vaccine strains A/Texas/36/1991 and B/Panama/45/1990 in young (P <0.0001 A/Texas and B/Panama) and older adults (P = 0.0002 A/Texas, P <0.0001 B/Panama) following vaccination, corroborating with the HAI responses (Fig. 1E and 3A). IIV also boosted neutralizing antibodies against future H1N1 (A/California/7/2009) in young adults (P = 0.0089), and against future IBV strain (B/Brisbane/60/2008) in both age groups (P = 0.0002 young adults, P = 0.0078 older adults) (Fig. 3A). Geometric mean titer (GMT) antibody landscapes within young and older adults showed how little boosting occurred against future H3N2 strains in comparison to more prominent future boosting against multiple future H1N1 and IBV strains following vaccination (Fig. 3B), further highlighting the need to improve vaccine strategies for H3N2, especially for older adults at risk of life-threatening influenza.

Divergent antibody response signatures were observed between younger and older adults

The multidimensional systems serology approach can comprehensively define antibody responses including their isotype, subclass, and effector function to a range of different antigens. We developed a multiplex antigen array that included 14 influenza antigens (8 HA, 3 neuraminidase (NA) and 3 nucleoprotein (NP) proteins) from the 1994 vaccine strains and future virus strains (fig. S2 and table S2) to characterize vaccine-induced and cross-reactive antibody responses. These experiments assessed plasma from 35 younger and 38 older adults, with 28 participants per age group overlapping with the HAI antibody landscape cohort. Each of the 14 influenza antigens were assessed for the presence of 12 different antibody responses

including total IgG, IgM isotypes, Ig subclasses (IgG1, IgG2, IgG3, IgG4, IgA1) and Fc gamma receptors (FcγIIa-H131, FcγRIIa-R131, FcγRIIb, FcγRIIIa-V158 and FcγIIIa-F158, data file S1), making up a total of 168 features. Antibody binding to Fc receptors on immune cells can lead to antibody-dependent cellular phagocytosis (FcγRIIa, i.e. CD32a) and antibody-dependent cell-mediated cytotoxicity (FcγIIIa, i.e. CD16) of target cells.

Changes in antibody expression levels as median fluorescence intensity (MFI) to each influenza antigen were summarized by volcano plots (Fig. 4, A to D, fig. S3, A to D) to compare antigen-antibody feature responses between timepoints for each age group and between age groups for i) all antigens (Fig. 4, A to D), ii) 1994 vaccine antigens (H1-HA A/Texas/36/1991 and H3-HA A/Beijing/32/1992) (fig. S3, A and C), or iii) post-1994 antigens in the analyses (fig. S3, B and D, table S2). When comparing differences between baseline versus d28 post-vaccination, most responses increased post-vaccination for both age groups ($P < 0.05$), with only a few IgM responses enriched at baseline (Fig. 4, A and B, fig. S3, A and B). Spider plot analyses also showed higher median MFI values for some responses in younger and older adults at d28 compared with baseline ($P < 0.05$; data file S1), which overlapped for H1 and IBV antigens (fig. S4). Analyses of features between age groups at either timepoints revealed dominant skewing of responses towards older adults (Fig. 4, C and D), particularly at baseline and against future antigens, whereas minimal enrichment of features was observed in older adults when only the 1994 vaccine antigens were analyzed (Fig. 4, C and D, and fig. S3, C and D).

To further probe the qualitative differences between age groups observed at baseline, LASSO (least absolute shrinkage and selection operator) regression and Principal Component Analysis (PCA) were performed on the baseline dataset including age as a feature variable. For the 1994 vaccine antigens analysis, pre-vaccination baseline antibody responses revealed two distinct clusters between younger and older adults (Fig. 4E), which separated diagonally across PC2 based on selection of 6 out of 73 features (Fig. 4F). Older adults had stronger baseline Fc-receptor and IgA1 responses to the vaccine antigens, indicating a more mature baseline immune profile prior to vaccination, whereas younger adults exhibited IgM responses characteristic of naïve antibody responses. Baseline responses against future antigens were selected from 10 out of 145 variable features revealing clear clustering of age groups diagonally across PC2 (Fig. 4, G and H), which was similar to their baseline responses against vaccine antigens. This future antigen analysis suggested a more divergent cross-reactive signature in older adults which featured mature IgA1 responses, whereas younger adults featured naive IgM responses prior to vaccination (Fig. 4, G and H). These divergent pre-vaccination signatures between younger

and older adults were also reflected in our all antigen analysis including all 168 variable features plus age (fig. S5, A and B). Analyses between timepoints (baseline versus d28) showed partial clustering across PC1 for both age groups, with almost all features associated with post-vaccination responses (fig. S5, C to F), supporting our volcano plot analyses. Taken together, our systems serology data revealed qualitative differences occurring prior to vaccination between younger and older adults in response to vaccine antigens and future antigens, with older adults exhibiting more mature immune responses.

1994 IIV vaccination elicited cross-reactive memory B cells that bound future H1 and IBV HA-probes

To define influenza-specific B cell memory responses, fluorescently-labeled recombinant HA-probes were custom generated for H1, H3, and IBV HAs from the 1994 vaccine strains (fig. S6). To detect cross-reactive responses against future strains, HA-probes representing two future vaccine strains for each subtype were included (fig. S7, A to C and table S3). These were H1-HA-probes from A/Brisbane/59/07 (2009 IIV) and A/Victoria/2570/2019 (H1N1)pdm09-like (2021-2022 IIV), H3-HA-probes from A/Perth/16/2009 (2010-2012 IIV) and A/Switzerland/9715292/2013 (2015 IIV), and IBV-HA-probes from B/Brisbane/60/2008 (2010-2012, 2016-2017 IIV) and B/Phuket/3073/2013 (2015, 2018-2025 IIV).

Despite 30 years of cryopreservation, viability of these historic PBMC samples was high, averaging 89-92% for both groups (Fig. 5A). For the 1994 vaccine strains, H1-HA Texas$^+$ memory B cells increased 5.4-fold in young adults following vaccination ($P < 0.0001$) and 1.9-fold higher in older adults ($P = 0.0033$) (Fig. 5, B and C). Vaccine-driven Texas$^+$ frequencies were higher in younger adults compared with older adults ($P = 0.0395$). H3-HA Beijing$^+$ memory B cells responses were very low in frequency (<0.1%) and did not significantly increase for either group. Although we did observe vaccination-induced responses in a subset of individuals, where 19 out of 39 younger adults (49%) and 17 out of 39 older adults (44%) had increased H3-Beijing$^+$ memory B cell responses (average 2.6-fold and 2.1-fold increases, respectively) (fig. S7D). IBV-HA Panama$^+$ memory B cells responses increased in both younger and older adults following vaccination (3.8-fold and 2.3-fold, respectively; $P < 0.0001$) with older adults having higher baseline frequencies compared with younger adults ($P < 0.001$).

To detect cross-reactive H1-specific memory B cell responses, H1-HA probes were initially split into two panels of Texas$^+$Bris/07$^+$ and Texas$^+$Vic/19$^+$ (Fig. 5D). Further optimization of H3-HA and IBV-HA probes allowed us to include 3 probes in a single staining

panel (fig. S8 and table S3). Although at lower frequencies, we observed increased responses in H1-cross-reactive Texas$^+$Bris/07$^+$ memory B cells in both younger and older adults following vaccination ($P = 0.0010$ and $P = 0.0290$, respectively), but not for the Texas$^+$Vic/19$^+$ memory B cell response (Fig. 5E). Patterns were reflected in total Bris/07$^+$ and Vic/19$^+$ memory B cell responses (fig. S8, A and B). Given H3-HA Beijing$^+$ memory B cell responses were <0.1%, we did not detect any cross-reactive H3-specific B cells. Rather, single-positive H3-Perth$^+$ memory B cells were detected in both groups at baseline but did not in general increase following vaccination (fig. S8, C and D). However, we observed increased responses in H3-Switz$^+$ memory B cells in younger adults ($P = 0.0011$, 3.1-fold), although very low frequencies were detected (<0.1%) (fig. S8, C and D).

Cross-reactive IBV-HA-specific memory B cells responses towards the Yamagata lineage strains were also observed, with increases in Panama$^+$Phuket$^+$ memory B cells in both young (10.9-fold) and older adults (2.9-fold) following vaccination (Fig. 5, F and G). This was reflected in the total Phuket$^+$ memory B cell response (fig. S8, E and F). IBV Bris$^+$ memory B cells from the Victoria lineage were detected in both age groups but did not increase following vaccination (fig. S8, E and F) or cross-react with the Yamagata probes.

To assess the presence of cross-reactive stalk-specific memory B cell responses, dual staining with group 1 (H1 and H5) and group 2 (H3 and H7) HA-specific probes was performed on a subset of younger and older adults (Fig. 5H and fig. S9). H5-specific memory B cell responses increased following vaccination in younger adults ($P = 0.0156$), but not for older adults (Fig. 5I). H7-specific memory B cell responses were also detected but did not increase following vaccination in both age groups. Group 1 H1/H5 cross-reactive B cells were detected at lower cell events but showed increases in older adults ($P = 0.0195$), whereas group 2 H3/H7 cross-reactive B cells were not detected (Fig. 5J).

Phenotype (CD21 and CD27 expression) and isotype composition of total B cells did not change following vaccination, with the exception of young adults who had a small decrease in CD21$^-$CD27$^-$ B cells (Fig. 6A). At baseline and d28, younger adults had more IgD$^+$IgM^{low} B cells ($P < 0.05$) and less IgM$^+$ B cells ($P < 0.01$) compared with older adults (Fig. 6B). In contrast, for HA-specific B cells, we observed prototypical increases in the proportion of the activated memory CD21$^-$CD27$^+$ population for H1-Texas$^+$ and IBV-Panama$^+$ following vaccination, which coincided with a reduction in the resting memory CD21$^+$CD27$^+$ population (Fig. 6C). Cross-reactive H1 and IBV responses also showed similar activation patterns following vaccination, significant for the Panama$^+$Phuket$^+$ memory B cell response from older adults ($P < 0.01$) (Fig. 6D) and single probe analyses for H1-Bris/07$^+$, H1-Vic/19$^+$ and IBV-

Phuket$^+$ memory B cells ($P < 0.05$) (fig. S8G). Single-positive H3-Switz$^+$ memory B cells, although at very low frequencies, also showed increased activation phenotype in both age groups ($P < 0.01$) (fig. S8G). In terms of isotype, HA-specific B cells were predominantly IgG$^+$ for H1 and IBV responses, and IgA$^+$/IgE$^+$ for H3 responses, profiles of which did not change following vaccination (Fig. 6, E and F, and fig. S8H). Phenotypes and isotypes of H5- and H7-specific memory B cells were also unchanged following vaccination (Fig. 6, G and H. Similarly, patterns were unchanged for cross-reactive H1/H5 stalk-specific memory B cells, which were mainly of IgG$^+$ isotype (Fig. 6, I and J).

Broad antibody and B cell responses were generated following 1994 IIV vaccination

We generated correlation matrices of HAI titers, microneutralization titers, systems serology data, and virus-specific memory B cell responses across vaccine strains A/Texas/36/1991, A/Beijing/32/1992, and B/Panama/45/1990 responses following IIV across young and older adults. For responses against H1N1 A/Texas/36/1991, we observed positive correlations between HAI, isotype, and Fc binding, as well as virus-neutralizing antibody responses, across both young and older adults, suggesting high quality H1N1 antibody responses across age (Fig. 7A). Although older adults had fewer positive correlations between isotype and Fc binding. In younger adults, antigen-specific memory B cells positively correlated with bulk IgA and IgM antibody responses, as well as IgG-specific memory B cell responses.

Antibody responses against vaccine strain H3N2 A/Beijing/32/1990 in younger adults positively correlated with Fc binding, consistent with our observation on H1N1 responses. IgG2 in young adults negatively correlated with total IgG, IgG1 responses, and Fc binding (Fig. 7B). We did not observe any correlations between antibody and B cell responses towards H3N2 vaccine strain in younger and older adults. However, we detected positive correlation between HAI titers, neutralizing antibody titers, and B/Panama-specific CD27$^+$CD21$^-$ B cell responses towards vaccine strain IBV B/Panama/45/1990 in young adults, but only found positive correlations between virus neutralizing antibody titers and HAI antibody responses in older adults (Fig. 7C).

DISCUSSION

In our study, we aimed to define pre-existing antibody and memory B cell responses elicited by influenza vaccination against future influenza virus strains. We analyzed historic influenza vaccination cohorts of young and older adults from 1994 and assessed future immune responses

spanning three decades of differentially evolving influenza subtypes encompassing H1N1, H3N2, and IBV. Our main findings showed that, following vaccination, antibody responses increased against all three 1994 vaccine strains in young and older adults; that high-quality vaccine-induced antibody responses were achieved in both age groups, but divergent signatures existed against future antigens; and that antibody responses and cross-reactive memory B cell responses increased against future H1N1 and IBV strains, including the presence of group 1 cross-reactive H1/H5-specific B cell responses, but were less evident for the future H3 and group 2 H7N9 strains.

Our multiplex data provide a sensitive approach to measure the quality of antibody responses against the vaccine and future antigens. We and others have previously shown that multiplex serology (when appropriately validated) robustly correlates with antibody titers quantified via ELISAs and other serological assays for multiple pathogens including influenza virus (*19, 20*), HIV (*21*), and SARS-CoV-2 (*22, 23*). Our data suggested that clustering was more impacted by Ig subtype and Fc effector function, and less so by the antigen sub-strain. Prior to vaccination, older adults had features of IgA1 and FcγRII antibody responses, representing more mature responses, whereas younger adults had features of naïve IgM responses. Post-vaccination, however, there were minimal differences in antibody responses against all antigens between younger and older adults, representing high quality vaccine-specific responses in both age groups.

Our antibody landscape data revealed modest increases in responses to multiple H1 and IBV future strains in both young and older adults following 1994 vaccination. Four older participants who were born in the late 1910s and early 1920s may have been infected as a child with the 1918 H1N1 pandemic strain, which closely resembles the 2009 pandemic strain. These were the only participants seropositive for A/California/7/2009 or A/Michigan/45/2015 at baseline (HAI of 40 and above) with the eldest (75 years old) having a boosted A/California/7/2009 response; in contrast, none of the younger adults were seropositive for these future strains at baseline. Vaccination did, however, generate antibody responses against either A/California/7/2009 or A/Michigan/45/2015 in three younger adults above the positivity threshold, which coincided with high antibody responses towards the vaccine A/Texas/36/1991 strain. In addition, although we observed that both age groups generated neutralizing antibody responses against the vaccine A/Texas/36/1991 strain, only young adults had neutralizing antibodies against future A/California/7/2009. This suggests that in some young individuals, vaccination can elicit neutralizing cross-reactive antibody responses between the vaccine

subtype strain and future strains whereas older adults had less ability to neutralize future H1 strains. These results corroborate previous vaccination studies demonstrating that influenza vaccination can induce broadly cross-reactive neutralizing antibodies against both current and historical subtypes (*24, 25*).

We provide evidence of cross-reactive antibody responses between the two IBV lineages in both young and older adults who were potentially exposed to either lineage before the 1980s, as well as cross-reactive neutralizing antibodies against the vaccine strain and against future Victoria-lineage. In our 1994 vaccine study, our younger adults, born mainly in the early 1970s, had less exposure to IBV than our older adults, born in the 1920s, who experienced IBV strains since the 1940s. Recent investigations by Edler *et al*. (*14*) revealed that birth cohorts between 1980s to late 1990s, when Yamagata strains predominated, exhibited the highest antibody titers against future Yamagata-lineage strains, which were two-fold higher than antibody levels against future Victoria-lineage strains. In contrast, earlier birth cohorts (1940-1980) demonstrated cross-reactivity to future Victoria-lineage strains, corroborating our findings (*14*). In addition, our correlation matrix analysis showed that HAI antibody responses correlated with neutralizing antibody responses against vaccine H1N1 and IBV strains across both age groups, indicating the overall increase in antibody level, neutralizing capability, and Fc binding ability.

Supporting the antibody landscape data, both age groups showed prominent increases in vaccine-probe$^+$ cross-reactive memory B cell responses against H1N1 A/Brisbane/59/2007 and B/Phuket/3073/2013, and in some individuals, increased cross-reactive responses against the A/Victoria/2570/2019 (H1N1)pdm09-like strain were observed. Although antibody responses against A/Brisbane/59/2007 were below the seropositivity threshold for both age groups, the presence of H1N1-Texas$^+$Brisbane$^+$ memory B cells revealed that vaccination can also generate cross-reactive memory B cell responses targeting non-neutralizing epitopes. Additionally, the presence of H1 stem antibodies supports our findings of non-neutralizing stalk responses in the cross-reactive H1 Texas$^+$/Brisbane$^+$ memory B cell responses. In our 1994 cohorts, we could only detect cross-reactive Yamagata-lineage Panama$^+$Phuket$^+$ memory B cell responses or single-positive Victoria-lineage Brisbane$^+$ memory B cells, including in the young participants who had antibody responses to both lineages. In contrast, we have previously shown that cohorts sampled during the mid-2010s have highly cross-reactive antibody and memory B cell responses to both lineages (*26*). The presence and boosting of group 1 H1/H5-cross-reactive stalk-specific memory B cell responses were observed in our cohort, potentially contributing to the cross-reactive H1-specific B cell response. However, we

did not detect any group 2 cross-reactive-H3/H7-specific B cells, supporting the lower levels of H3 stem antibodies observed in our cohort. Our findings thus provide evidence for boosting and generation of vaccine-specific and cross-reactive memory B cell responses, particularly for H1 and IBV future strains. The change in activation phenotype, but not isotype following vaccination, represents a prototypical response in agreement to our previous study comparing influenza-specific memory B cell responses following influenza virus infection versus vaccination (*18*). Cross-reactive stalk-specific H1 responses were also boosted following vaccination, although not for H3, which may explain why H3 responses were minimal towards future virus strains compared with H1 responses.

Although we observed vaccination-induced HAI antibody responses to the H3 A/Beijing/32/1992 vaccine strain, we did not consistently observe increases in the HA Beijing^{+} memory B cell response, with increased responses only observed in a subset of individuals. We acknowledge that different recombinant HA-probes can vary in their ability to identify HA-specific B cell populations. Therefore, the H3-Beijing probe was variable in detecting all the memory B cells responses, as the frequencies of HA Beijing^{+} memory B cells were very low (most below 0.05%) compared with the other vaccine probes.

Seasonal vaccination, even within this historical cohort, appears primarily driven by recall of immune memory established via previous influenza infection or immunization. This was particularly evident in our observed recall of highly cross-reactive antibody and B cell responses, which are primarily localized within the HA stem region of high conservation (*27*). Previous studies have established that cross-reactive stem-directed humoral immunity is widespread in human populations (*28, 29*), particularly for epitopes shared within Group 1 influenza A viruses (i.e., H1N1, H5N1) (*30*). Such immunity is readily recalled upon subsequent exposure to both seasonal vaccines (*31*) and vaccines against pandemic influenzas (*32-34*). However, it should be considered that the memory recall responses observed in our study may not remain at sufficient levels to provide protection thirty years later, as the cross-reactive responses were measured during the peak of circulating antibodies and B cells in 1994.

Immunization also facilitates recall of responses to cross-reactive epitopes in the HA head domain, including within epitopes capable of mediating broad HAI activity (*35, 36*). However, the degree of cross-reactive conservation is generally less than epitopes in the stem and highly influenced by antigenic drift within circulating viruses. We found less evidence of recall of H3N2-specific responses, in line with previous reports (*37*), likely related to the increased phylogenetic and antigenic diversity within this subtype relative to H1N1 or IBV. Future studies might utilize modern structural techniques like electron microscopy polyclonal

epitope mapping (*38*) to better define antigenic sites enabling broad neutralizing activity against unencountered viruses. Furthermore, the study of influenza immunity in adults is necessarily complicated by the ubiquitous pre-existing immunity established by past infection and immunization. Although the recall of immune memory predominates in the response to seasonal influenza vaccines, this can in turn dampen primary responses to vaccine antigens leading to potential reductions in serological titers, a phenomenon often termed "original antigenic sin" (OAS). The complicated interplay of prior immunity and influenza is discussed in more detail elsewhere (*39*).

There were limitations to our study. The multiplex bead array assay had no commercially available proteins to measure systems serology responses to the 1994 IBV/Panama vaccine antigens. We acknowledge that different recombinant HA-probes can vary in their ability to identify HA-specific B cell populations, which is another limitation. Additionally, the microneutralization assay does not accurately measure HA stalk antibodies as a correlate of immune protection compared with plaque-reduction assays and should be interpreted with caution.

Thus, using our historic 1994 vaccinated cohort, we provide evidence for boosting of vaccine-specific and cross-reactive memory B cell responses, particularly for H1 and IBV future strains. Conversely, we showed reduced H3N2 responses against future influenza strains spanning three decades. Considering the recent influenza epidemic outbreak of suspected H3N2 in Japan (6,013 cases since 10th October 2025) (*40*), there is an unmet need for improved preventative measures and vaccination strategies to better protect vulnerable populations from life-threatening illness, especially towards H3N2.

MATERIALS AND METHODS

Study design

The 1994 cohort was established as part of a Phase IV study to evaluate immune responses to the 1994 IIV (FLUVAX, CSL Limited, Melbourne Australia) during April 1994, in a younger adult cohort aged less than 60 years (n = 89, 18-53 years) and an older adult cohort aged 60 years and above (n = 68, 60-75 years). Although current recommendations for influenza vaccinations for older adults are cut-off at 65 years and above, the median age of the older cohort was 69 years and so the majority of this group was 65+ years, reflective of an older adult cohort. The exclusion criteria included individuals who were vaccinated against influenza since June 1993. Only prior vaccination history was collected for the younger adults. Blood was

collected at day 0 prior to vaccination and between days 24-32 post-vaccination. Plasma was stored at -20ºC or below for serological assays. PBMCs were cryopreserved at -196ºC for cellular assays. All participants provided written informed consent. Study was approved by the Royal Melbourne Institute of Technology Ethics Committee (#40/93 and #41/93) and the University of Melbourne Human Research Ethics Committee (#13344 and #31236).

The objective of this study was to use samples from the 1994 cohort to define pre-vaccination antibody reactivity as well as antibody and B cell responses elicited by 1994 influenza vaccination against future influenza virus strains. Samples were selected for each experiment based on sample availability to have the most overlap of the same individuals within different experiments for correlative analyses. A sample size of at least 28 per group was sufficient to detect a large effect size between two groups ($\alpha = 0.05$ and a power of 0.8). For PBMC experiments, samples were used once with one vial available. Assays using plasma were performed once, except in duplicate as technical replicates for multiplex assays.

Antibody landscapes

Viruses for HAI assays were obtained from WHO Collaborating Centre for Reference and Research on Influenza and CSL Seqirus Ltd. A list of viruses is detailed in table S1. Phylogenetic trees were constructed using Neighbor-Joining tree build method, with Jukes-Cantor genetic distance model, by Geneious Prime software 2025.0.3. HAI antibody landscapes against the vaccine strain and other influenza strains from table S1 were measured at the WHO Collaborating Centre for Reference and Research on Influenza. Plasma samples were treated with receptor destroying enzyme (Denka Seiken) to remove non-specific inhibitors of agglutination then adsorbed with a mixture of guinea pig and turkey red blood cells to remove non-specific agglutination. Serial two-fold dilutions of plasma from 1:10 to 1:10240 were incubated with virus at 4 HA units/25 µl for 30 minutes followed by addition of 1% red blood cells from either guinea pigs for H3N2 viruses or turkeys for H1N1 and IBV viruses. Assays were performed in 96-well U-bottom or V-bottom plates for guinea pig and turkey red blood cells, respectively, and incubated for 30 minutes and 90 minutes, respectively. Antibody titers were read as the highest dilution with complete inhibition of agglutination using an automated plate reader (CypherOne, InDevR). When calculating geometric mean titers (GMTs) for pre and post-vaccination titers in younger and older adult groups, a maximum-likelihood approach to account for nondetectable titers (e.g. <10) was used as described (*41*), and implemented using the "gmt" function from the titertools R package (*42*).

Expression of recombinant influenza HA proteins

Recombinant HA and HA stem proteins used in ELISAs were produced as previously described (*26, 33, 43, 44*). For influenza A, DNA encoding the HA ectodomains for H1N1 (A/Texas/36/1991, A/Brisbane/59/2007, A/Victoria/2570/2019), H3N2 (A/Beijing/32/1992, A/Beijing/32/1992, A/Perth/16/2009, A/Switzerland/9715292/2013), H5N6 (A/Fujian-Sanyuan/21099/2017) and H7N9 (A/Shanghai/01/2013) were synthesized (GeneArt/Thermo Fisher) and cloned into mammalian expression vectors upstream from a T4 "foldon" trimerization domain, Avitag biotinylation site and N-terminal polyhistidine tag. All influenza A HA proteins were engineered with a Y to F mutation within the receptor-binding site (position 95-98 depending on the strain) which abolishes binding to cell-surface sialic acids (*33*). DNA encoding stabilized stem proteins for influenza A H1 (derived from A/California/04/2009) (*44*) and H3 (derived from A/Finland/486/2004) (*43*) were similarly cloned onto expression vectors with the same N-terminal Foldon-Avitag-HIS. For influenza B (B/Panama/45/1990, B/Brisbane/60/2008, B/Phuket/3073/2013), DNA encoding unmodified HA ectodomains were similarly cloned. All HA and HA stem proteins were expressed by transient transfection of Expi293 cells (#A14527, Life Technologies, Thermo Fisher Scientific), purified by polyhistidine-tag affinity and size exclusion chromatography and stored at -80ºC. For use as flow cytometric probes, HA proteins were biotinylated using a BirA site directed kit (Avidity) and prior to use labeled via the sequential addition of streptavidin conjugated to PE (Thermo Fisher #S866), allophycocyanin (APC, Thermo Fisher #S868), BV711 (BD #563262) or brilliant violet (BV) 421 (BD #563259).

Stem Antibody ELISA

Antibody binding to HA stem proteins derived from H1N1 A/California/04/2009 and H3N2 A/Finland/486/2004 was tested by ELISA as previously described (*45*), where antigenicity of the stabilized influenza HA stem proteins was established using panels of stem-specific monoclonal antibodies. Briefly, 96-well ImmunoSorp plates (Thermo Fisher Scientific) were coated overnight at 4°C with 2 μg/ml recombinant HA stem, before blocking with 1% fetal calf serum in phosphate-buffered saline (PBS). Plasma was serially diluted 4-fold (1:30 to 1:491520) before addition and incubated for 2 hours at room temperature, prior to detection with 1:20,000 dilution of HRP-conjugated rabbit anti–human IgG (Dako) for 1 hour at room temperature. Plates were washed and developed using tetramethylbenzidine (TMB) substrate

(Invitrogen), stopped with 0.12M sulfuric acid, and read at 450 nm on a Fluostar Omega (BMG Labtech). Endpoint titers were calculated using a fitted curve (4 parameter log regression) and a cut-off of 2x background absorbance using GraphPad Prism v10 software.

Microneutralization assays

Microneutralization (MN) assays were conducted according to WHO protocols (*46, 47*) using MDCK cells (#CCL-34, ATCC), and plasma treated as per the HAI assay protocol above. Assays were performed in 96-well flat-bottom tissue culture plates. Plasma samples were serially diluted two-fold (1:10 to 1:10240) in DMEM (Gibco) supplemented with 1% bovine serum albumin (Sigma-Aldrich), 25 mM HEPES (Gibco), 100 U/ml penicillin-streptomycin solution (Gibco), and 2 µg/ml TPCK-treated trypsin (Worthington Biochemical), then incubated with 200 $TCID_{50}$/50 µl virus at 37°C/5% CO_2. After one hour, $1.5x10^4$/100 µl MDCK cells were added to virus-plasma mixtures before plates were incubated for 18-20 hours at 37°C/5% CO_2. The following day, cell monolayers were washed with 0.05% Tween 20 (Sigma Aldrich) in PBS and fixed with 80% acetone. The amount of infection was evaluated through an ELISA readout. Presence of virus was detected using murine monoclonal antibodies kindly gifted by CSL Seqirus Ltd. Anti-type A and B nucleoprotein antibodies (diluted 1:1,000 and 1:10,000, respectively) were added at 100 µl per well and incubated for 1 hour, followed by 100 µl HRP-conjugated goat anti-mouse IgG antibody (Invitrogen; 1:1000) for 1 hour. Plates were washed then developed by addition of 100 µl KPL TMB Peroxidase Substrate (Seracare) and reaction was stopped by addition of 100 µl 1M HCl. Absorbance was measured at 450 nm using the FLUOStar Omega microplate reader (BMG Labtech). The midpoint OD value between wells containing virus only and wells containing cells only was used as a cutoff for neutralization activity. Test wells with an OD_{450} below or equal to the cutoff were considered positive for neutralization activity. The virus neutralization antibody 50% titer was defined as the reciprocal of the highest dilution that yielded positive neutralization activity.

Multiplex bead array assay

A customized influenza 16-plex bead array was generated including his-tagged influenza proteins (HA, NA, NP) coupled to magnetic carboxylated beads (table S2). Successful coupling of antigens was confirmed by his-tag antibody staining, as previously described (*48*). SIV gp120- and Tetanus-coupled beads were included as negative and positive control antigens, respectively. Validation of the multiplex bead array included strong correlation (fig. S2A) and confirmation that there were no differences in median fluorescence intensity (MFI) values

between single-plex and multiplex arrays (fig. S2B). The optimal plasma dilution was validated by strong correlation of ED_{50} responses, defined by half-maximal effective dilution, with MFIs of the chosen single dilution and selected for suitability across detectors and antigens (fig. S2, C and D), as previously described (*23, 49*). Plasma samples were diluted 1:200 in PBS before incubating 1:1 (final dilution 1:400) with antigen-coupled beads. The optimal plasma dilution was validated by correlation of ED_{50} responses with responses at the chosen single dilution and selected for suitability across detectors and antigens (fig. S1). The following day, samples were incubated with soluble FcγR dimers or mouse anti-human detector antibodies that were either phycoerythrin (PE)-conjugated or biotinylated, followed by incubation with streptavidin-PE for biotinylated detection reagents (table S4), before reading on an Intelliflex Luminex instrument system (Luminex), as described (*48*). Samples were run in duplicate as technical replicates.

HA-specific B cell responses

Vaccine-boosted and cross-reactive memory B cell responses were measured by flow cytometry (fig. S8 and S9) using a panel of in-house fluorescently labeled recombinant HA-probes comprising the 1994 IIV strain and two future strains for H1, H3, and IBV groups. PBMC samples were split across the three groups (n = 18-30 per group). PBMCs were thawed in warm RPMI media (Thermo Fisher), stained with HA probes in PBS (60 ng per probe per test, except for B/Panama/45/1990 which used 12 ng per test) and antibody panels as described in table S3 and table S5 for 30 mins on ice, then fixed with 1% paraformaldehyde diluted in MACS buffer (PBS with 0.5% (w/v) bovine serum albumin and 2mM EDTA, pH8.0) and acquired immediately on a LSR Fortessa (BD Biosciences), as previously described (*9, 18*). For H1N1, samples were split into two staining panels of A/Texas/36/1991 and A/Brisbane/59/2007 recombinant HA-probes, and A/Texas/36/1991 and A/Victoria/2570/2019 (H1N1)pdm09-like recombinant HA-probes (young n = 19, older n = 18). For H3 and IBV panels (n = 0 per age group), all three probes were included in one staining panel. A subset of PBMCs (n = 10 per age group, including 8-9 new participants) were also stained for group 1 (H1/H5) and group 2 (H3/H7) comparisons using H1N1 A/Texas/36/1991 versus H5N6 A/Fujian-Sanyuan/21099/2017 and H3N2 A/Beijing/32/1992 versus H7N9 A/Shanghai/01/2013 (table S3). For all experiments, PBMCs were stained between 1.0 and $5.5x10^6$ cells per panel.

Statistical analysis

GraphPad Prism v10 software was used to determine significance ($P < 0.05$) of nonparametric datasets (two-tailed) for Mann-Whitney U-test (unpaired) and Wilcoxon sign-rank test (paired) for comparisons between two groups, and Tukey's multiple comparison test to compare row means between more than two groups. Median and interquartile range (IQR) or mean and standard deviation (SD) were also constructed by GraphPad Prism. To estimate optimal dilutions to run multiplex assays, ED_{50} was calculated using four parameter dose-response curves with GraphPad Prism v10 software. For multiplex data, differences (z score group A - z score group B) between each feature from pre- to post-vaccination were determined by Wilcoxon matched-pairs signed rank test, and between age cohorts by Mann-Whitney U test, using the rstatix package (v0.7.2). The Holm correction for multiple comparisons was made; unadjusted $-\log_{10} P$ values are plotted, with the horizontal threshold line plotted at an adjusted ($-\log_{10}$) P value of 0.05. For validation of multiplex bead assays, Pearsons correlations were conducted between single and multiplex arrays. Volcano plots were plotted in R version 4.4.1 using the EnhancedVolcano package (v1.22.0). MFI values were right shifted by 1, then $\log_{10}$ transformed using the formula $\log_{10}(\text{MFI} + 1)$, and z score scaled for each analysis comparison. To transform the multiplex data for spiderplots (fig. S4), the median of each cohorts' antigen-specific detector MFI response was divided by the 98th percentile MFI value for each antigen-specific detector (98th percentile was chosen to minimize the impact of outliers). For multivariate analysis, data (y) was log-transformed ($y = \log_{10}(x + 1)$) before being normalized by mean centering and variance scaling of each feature. LASSO regression and PCA were performed and visualized using MATLAB (MathWorks), as previously described (*23, 50*). Frequency of selected samples was considered as the criteria of variable importance. Resampling of data were performed via 10-fold cross-validation and repeated 1,000 times (*48*). Figures were graphed using Prism (GraphPad). For correlation plots in Fig. 7, HAI and microneutralization titers were $\log_2$ transformed, and systems serology MFI values were $\log_{10}$ transformed as described for the multiplex bead array assay. Spearman's rank correlation was calculated using the R package psych (2.4.12), with P-values adjusted for false discovery rate (FDR). Only correlations with FDR < 0.05 were plotted using corrplot (version 0.95). All individual level data for $n < 20$ are presented in data file S2.

List of Supplementary Materials

Fig. S1 to S8

Table S1 to S5

MDAR Reproducibility Checklist

Data file S1 and S2

REFERENCES AND NOTES

1. C. Henry, N. Y. Zheng, M. Huang, A. Cabanov, K. T. Rojas, K. Kaur, S. F. Andrews, A. E. Palm, Y. Q. Chen, Y. Li, K. Hoskova, H. A. Utset, M. C. Vieira, J. Wrammert, R. Ahmed, J. Holden-Wiltse, D. J. Topham, J. J. Treanor, H. C. Ertl, K. E. Schmader, S. Cobey, F. Krammer, S. E. Hensley, H. Greenberg, X. S. He, P. C. Wilson, Influenza Virus Vaccination Elicits Poorly Adapted B Cell Responses in Elderly Individuals. *Cell Host Microbe* **25**, 357-366 e356 (2019).
2. S. Zhu, J. Quint, T. Leon, M. Sun, N. J. Li, C. Yen, M. W. Tenforde, B. Flannery, S. Jain, R. Schechter, C. Hoover, E. L. Murray, Estimating Influenza Vaccine Effectiveness Against Laboratory-Confirmed Influenza Using Linked Public Health Information Systems, California, 2023-2024 Season. *J Infect Dis*, (2025).
3. Centers for Disease Control and Prevention (CDC), "Flu and People 65 Years and Older". *https://www.cdc.gov/flu/highrisk/65over.htm*, (2025).
4. C. A. DiazGranados, A. J. Dunning, M. Kimmel, D. Kirby, J. Treanor, A. Collins, R. Pollak, J. Christoff, J. Earl, V. Landolfi, E. Martin, S. Gurunathan, R. Nathan, D. P. Greenberg, N. G. Tornieporth, M. D. Decker, H. K. Talbot, Efficacy of high-dose versus standard-dose influenza vaccine in older adults. *N Engl J Med* **371**, 635-645 (2014).
5. A. Domnich, L. Arata, D. Amicizia, J. Puig-Barbera, R. Gasparini, D. Panatto, Effectiveness of MF59-adjuvanted seasonal influenza vaccine in the elderly: A systematic review and meta-analysis. *Vaccine* **35**, 513-520 (2017).
6. J. R. Chung, M. A. Rolfes, B. Flannery, P. Prasad, A. O'Halloran, S. Garg, A. M. Fry, J. A. Singleton, M. Patel, C. Reed, t. I. H. S. N. Us Influenza Vaccine Effectiveness Network, I. S. D. C. f. D. C. the Assessment Branch, Prevention, Effects of Influenza Vaccination in the United States During the 2018-2019 Influenza Season. *Clin Infect Dis* **71**, e368-e376 (2020).
7. S. G. Sullivan, M. B. Chilver, K. S. Carville, Y. M. Deng, K. A. Grant, G. Higgins, N. Komadina, V. K. Leung, C. A. Minney-Smith, D. Teng, T. Tran, N. Stocks, J. E. Fielding, Low interim influenza vaccine effectiveness, Australia, 1 May to 24 September 2017. *Euro Surveill* **22**, (2017).
8. F. Liu, F. L. Gross, S. N. Jefferson, C. Holiday, Y. Bai, L. Wang, B. Zhou, M. Z. Levine, Age-specific effects of vaccine egg adaptation and immune priming on A(H3N2) antibody responses following influenza vaccination. *J Clin Invest* **131**, (2021).
9. M. Koutsakos, A. K. Wheatley, L. Loh, E. B. Clemens, S. Sant, S. Nüssing, A. Fox, A. W. Chung, K. L. Laurie, A. C. Hurt, S. Rockman, M. Lappas, T. Loudovaris, S. I. Mannering, G. P. Westall, M. Elliot, S. G. Tangye, L. M. Wakim, S. J. Kent, T. H. O. Nguyen, K. Kedzierska, Circulating TFH cells, serological memory, and tissue compartmentalization shape human influenza-specific B cell immunity. *Science Translational Medicine* **10**, eaan8405 (2018).
10. M. Auladell, H. V. M. Phuong, L. T. Q. Mai, Y. Y. Tseng, L. Carolan, S. Wilks, P. Q. Thai, D. Price, N. T. Duong, N. L. K. Hang, L. T. Thanh, N. T. H. Thuong, T. T. K. Huong, N. T. N. Diep, V. T. N. Bich, A. Khvorov, L. Hensen, T. N. Duong, K. Kedzierska, D. D. Anh, H. Wertheim, S. D. Boyd, K. L. Good-Jacobson, D. Smith, I. Barr, S. Sullivan, H. R. van Doorn, A. Fox, Influenza virus infection history shapes antibody responses to influenza vaccination. *Nat Med* **28**, 363-372 (2022).
11. S. F. Andrews, Y. Huang, K. Kaur, L. I. Popova, I. Y. Ho, N. T. Pauli, C. J. Henry Dunand, W. M. Taylor, S. Lim, M. Huang, X. Qu, J. H. Lee, M. Salgado-Ferrer, F. Krammer, P. Palese, J. Wrammert, R. Ahmed, P. C. Wilson, Immune history profoundly affects broadly protective B cell responses to influenza. *Sci Transl Med* **7**, 316ra192 (2015).
12. S. F. Andrews, K. Kaur, N. T. Pauli, M. Huang, Y. Huang, P. C. Wilson, High preexisting serological antibody levels correlate with diversification of the influenza vaccine response. *J Virol* **89**, 3308-3317 (2015).
13. J. M. Fonville, S. H. Wilks, S. L. James, A. Fox, M. Ventresca, M. Aban, L. Xue, T. C. Jones, N. M. H. Le, Q. T. Pham, N. D. Tran, Y. Wong, A. Mosterin, L. C. Katzelnick, D. Labonte, T. T. Le, G. van der Net, E. Skepner, C. A. Russell, T. D. Kaplan, G. F. Rimmelzwaan, N. Masurel, J. C. de Jong, A. Palache, W. E. P. Beyer, Q. M. Le, T. H. Nguyen, H. F. L. Wertheim, A. C. Hurt, A. Osterhaus, I. G. Barr, R. A. M. Fouchier, P. W. Horby, D. J. Smith, Antibody landscapes after influenza virus infection or vaccination. *Science* **346**, 996-1000 (2014).
14. P. Edler, L. S. U. Schwab, M. Aban, M. Wille, N. Spirason, Y. M. Deng, M. A. Carlock, T. M. Ross, J. A. Juno, S. Rockman, A. K. Wheatley, S. J. Kent, I. G. Barr, D. J. Price, M. Koutsakos, Immune imprinting in early life shapes cross-reactivity to influenza B virus haemagglutinin. *Nat Microbiol* **9**, 2073-2083 (2024).

15. K. R. Short, K. Kedzierska, C. E. van de Sandt, Back to the Future: Lessons Learned From the 1918 Influenza Pandemic. *Front Cell Infect Microbiol* **8**, 343 (2018).
16. R. A. Medina, B. Manicassamy, S. Stertz, C. W. Seibert, R. Hai, R. B. Belshe, S. E. Frey, C. F. Basler, P. Palese, A. Garcia-Sastre, Pandemic 2009 H1N1 vaccine protects against 1918 Spanish influenza virus. *Nat Commun* **1**, 28 (2010).
17. T. K. Tsang, S. Cauchemez, R. A. Perera, G. Freeman, V. J. Fang, D. K. Ip, G. M. Leung, J. S. Malik Peiris, B. J. Cowling, Association between antibody titers and protection against influenza virus infection within households. *J Infect Dis* **210**, 684-692 (2014).
18. T. H. O. Nguyen, M. Koutsakos, C. E. van de Sandt, J. C. Crawford, L. Loh, S. Sant, L. Grzelak, E. K. Allen, T. Brahm, E. B. Clemens, M. Auladell, L. Hensen, Z. Wang, S. Nussing, X. Jia, P. Gunther, A. K. Wheatley, S. J. Kent, M. Aban, Y. M. Deng, K. L. Laurie, A. C. Hurt, S. Gras, J. Rossjohn, J. Crowe, J. Xu, D. Jackson, L. E. Brown, N. La Gruta, W. Chen, P. C. Doherty, S. J. Turner, T. C. Kotsimbos, P. G. Thomas, A. C. Cheng, K. Kedzierska, Immune cellular networks underlying recovery from influenza virus infection in acute hospitalized patients. *Nat Commun* **12**, 2691 (2021).
19. Z. N. Li, F. Liu, S. Jefferson, L. Horner, P. Carney, M. D. L. Johnson, J. P. King, E. T. Martin, R. K. Zimmerman, K. Wernli, M. Gaglani, M. Thompson, B. Flannery, J. Stevens, T. Tumpey, M. Z. Levine, Multiplex Detection of Antibody Landscapes to Severe Acute Respiratory Syndrome Coronavirus 2 (SARS-CoV-2)/Influenza/Common Human Coronaviruses Following Vaccination or Infection With SARS-CoV-2 and Influenza. *Clin Infect Dis* **75**, S271-S284 (2022).
20. H. A. Vanderven, S. Jegaskanda, B. D. Wines, P. M. Hogarth, S. Carmuglia, S. Rockman, A. W. Chung, S. J. Kent, Antibody-Dependent Cellular Cytotoxicity Responses to Seasonal Influenza Vaccination in Older Adults. *J Infect Dis* **217**, 12-23 (2017).
21. M. R. McLean, V. Madhavi, B. D. Wines, P. M. Hogarth, A. W. Chung, S. J. Kent, Dimeric Fcgamma Receptor Enzyme-Linked Immunosorbent Assay To Study HIV-Specific Antibodies: A New Look into Breadth of Fcgamma Receptor Antibodies Induced by the RV144 Vaccine Trial. *J Immunol* **199**, 816-826 (2017).
22. L. C. Rowntree, B. Y. Chua, S. Nicholson, M. Koutsakos, L. Hensen, C. Douros, K. Selva, F. L. Mordant, C. Y. Wong, J. R. Habel, W. Zhang, X. Jia, L. Allen, D. L. Doolan, D. C. Jackson, A. K. Wheatley, S. J. Kent, F. Amanat, F. Krammer, K. Subbarao, A. C. Cheng, A. W. Chung, M. Catton, T. H. Nguyen, C. E. van de Sandt, K. Kedzierska, Robust correlations across six SARS-CoV-2 serology assays detecting distinct antibody features. *Clin Transl Immunology* **10**, e1258 (2021).
23. K. J. Selva, C. E. van de Sandt, M. M. Lemke, C. Y. Lee, S. K. Shoffner, B. Y. Chua, S. K. Davis, T. H. O. Nguyen, L. C. Rowntree, L. Hensen, M. Koutsakos, C. Y. Wong, F. Mordant, D. C. Jackson, K. L. Flanagan, J. Crowe, S. Tosif, M. R. Neeland, P. Sutton, P. V. Licciardi, N. W. Crawford, A. C. Cheng, D. L. Doolan, F. Amanat, F. Krammer, K. Chappell, N. Modhiran, D. Watterson, P. Young, W. S. Lee, B. D. Wines, P. Mark Hogarth, R. Esterbauer, H. G. Kelly, H. X. Tan, J. A. Juno, A. K. Wheatley, S. J. Kent, K. B. Arnold, K. Kedzierska, A. W. Chung, Systems serology detects functionally distinct coronavirus antibody features in children and elderly. *Nat Commun* **12**, 2037 (2021).
24. M. G. Joyce, A. Wheatley, P. Thomas, G.-Y. Chuang, C. Soto, R. Bailer, A. Druz, I. Georgiev, R. Gillespie, M. Kanekiyo, W.-P. Kong, K. Leung, S. Narpala, M. Prabhakaran, E. Yang, B. Zhang, Y. Zhang, M. Asokan, J. Boyington, T. Bylund, S. Darko, C. Lees, A. Ransier, C.-H. Shen, L. Wang, J. Whittle, X. Wu, H. Yassine, C. Santos, Y. Matsuoka, Y. Tsybovsky, U. Baxa, J. Mullikin, K. Subbarao, D. Douek, B. Graham, R. Koup, J. Ledgerwood, M. Roederer, L. Shapiro, P. Kwong, J. Mascola, A. McDermott, Vaccine-Induced Antibodies that Neutralize Group 1 and Group 2 Influenza A Viruses. *Cell* **166**, 609-623 (2016).
25. F. Krammer, The human antibody response to influenza A virus infection and vaccination. *Nature Reviews Immunology* **19**, 383-397 (2019).
26. Y. Liu, H. X. Tan, M. Koutsakos, S. Jegaskanda, R. Esterbauer, D. Tilmanis, M. Aban, K. Kedzierska, A. C. Hurt, S. J. Kent, A. K. Wheatley, Cross-lineage protection by human antibodies binding the influenza B hemagglutinin. *Nat Commun* **10**, 324 (2019).
27. S. Nath Neerukonda, R. Vassell, C. D. Weiss, Neutralizing Antibodies Targeting the Conserved Stem Region of Influenza Hemagglutinin. *Vaccines (Basel)* **8**, (2020).
28. H. M. Yassine, P. M. McTamney, J. C. Boyington, T. J. Ruckwardt, M. C. Crank, M. K. Smatti, J. E. Ledgerwood, B. S. Graham, Use of Hemagglutinin Stem Probes Demonstrate Prevalence of Broadly Reactive Group 1 Influenza Antibodies in Human Sera. *Sci Rep* **8**, 8628 (2018).

29. J. Sui, J. Sheehan, W. C. Hwang, L. A. Bankston, S. K. Burchett, C. Y. Huang, R. C. Liddington, J. H. Beigel, W. A. Marasco, Wide prevalence of heterosubtypic broadly neutralizing human anti-influenza A antibodies. *Clin Infect Dis* **52**, 1003-1009 (2011).
30. D. Lingwood, P. M. McTamney, H. M. Yassine, J. R. R. Whittle, X. Guo, J. C. Boyington, C.-J. Wei, G. J. Nabel, Structural and genetic basis for development of broadly neutralizing influenza antibodies. *Nature* **489**, 566-570 (2012).
31. A. K. Wheatley, A. B. Kristensen, W. N. Lay, S. J. Kent, HIV-dependent depletion of influenza-specific memory B cells impacts B cell responsiveness to seasonal influenza immunisation. *Scientific Reports* **6**, 26478 (2016).
32. R. Nachbagauer, T. J. Wohlbold, A. Hirsh, R. Hai, H. Sjursen, P. Palese, R. J. Cox, F. Krammer, Induction of broadly reactive anti-hemagglutinin stalk antibodies by an H5N1 vaccine in humans. *J Virol* **88**, 13260-13268 (2014).
33. J. R. Whittle, A. K. Wheatley, L. Wu, D. Lingwood, M. Kanekiyo, S. S. Ma, S. R. Narpala, H. M. Yassine, G. M. Frank, J. W. Yewdell, J. E. Ledgerwood, C. J. Wei, A. B. McDermott, B. S. Graham, R. A. Koup, G. J. Nabel, Flow cytometry reveals that H5N1 vaccination elicits cross-reactive stem-directed antibodies from multiple Ig heavy-chain lineages. *J Virol* **88**, 4047-4057 (2014).
34. S. F. Andrews, M. J. Chambers, C. A. Schramm, J. Plyler, J. E. Raab, M. Kanekiyo, R. A. Gillespie, A. Ransier, S. Darko, J. Hu, X. Chen, H. M. Yassine, J. C. Boyington, M. C. Crank, G. L. Chen, E. Coates, J. R. Mascola, D. C. Douek, B. S. Graham, J. E. Ledgerwood, A. B. McDermott, Activation Dynamics and Immunoglobulin Evolution of Pre-existing and Newly Generated Human Memory B cell Responses to Influenza Hemagglutinin. *Immunity* **51**, 398-410.e395 (2019).
35. B. L. Tesini, P. Kanagaiah, J. Wang, M. Hahn, J. L. Halliley, F. A. Chaves, P. Q. T. Nguyen, A. Nogales, M. L. DeDiego, C. S. Anderson, A. H. Ellebedy, S. Strohmeier, F. Krammer, H. Yang, S. Bandyopadhyay, R. Ahmed, J. J. Treanor, L. Martinez-Sobrido, H. Golding, S. Khurana, M. S. Zand, D. J. Topham, M. Y. Sangster, Broad Hemagglutinin-Specific Memory B Cell Expansion by Seasonal Influenza Virus Infection Reflects Early-Life Imprinting and Adaptation to the Infecting Virus. *J Virol* **93**, (2019).
36. Y. Qiu, S. Stegalkina, J. Zhang, E. Boudanova, A. Park, Y. Zhou, P. Prabakaran, S. Pougatcheva, I. V. Ustyugova, T. U. Vogel, S. T. Mundle, R. Oomen, S. Delagrave, T. M. Ross, H. Kleanthous, H. Qiu, Mapping of a Novel H3-Specific Broadly Neutralizing Monoclonal Antibody Targeting the Hemagglutinin Globular Head Isolated from an Elite Influenza Virus-Immunized Donor Exhibiting Serological Breadth. *J Virol* **94**, (2020).
37. R. B. Abreu, G. A. Kirchenbaum, E. F. Clutter, G. A. Sautto, T. M. Ross, Preexisting subtype immunodominance shapes memory B cell recall response to influenza vaccination. *JCI Insight* **5**, (2020).
38. J. Han, A. J. Schmitz, S. T. Richey, Y. N. Dai, H. L. Turner, B. M. Mohammed, D. H. Fremont, A. H. Ellebedy, A. B. Ward, Polyclonal epitope mapping reveals temporal dynamics and diversity of human antibody responses to H5N1 vaccination. *Cell Rep* **34**, 108682 (2021).
39. J. W. Yewdell, J. J. S. Santos, Original Antigenic Sin: How Original? How Sinful? *Cold Spring Harb Perspect Med* **11**, (2021).
40. R. Fieldhouse, "Japan declares a flu epidemic — what this means for other nations". *Nature,* https://doi.org/10.1038/d41586-025-03367-z, (14 Oct. 2025).
41. S. H. Wilks, B. Muhlemann, X. Shen, S. Tureli, E. B. LeGresley, A. Netzl, M. A. Caniza, J. N. Chacaltana-Huarcaya, V. M. Corman, X. Daniell, M. B. Datto, F. S. Dawood, T. N. Denny, C. Drosten, R. A. M. Fouchier, P. J. Garcia, P. J. Halfmann, A. Jassem, L. M. Jeworowski, T. C. Jones, Y. Kawaoka, F. Krammer, C. McDanal, R. Pajon, V. Simon, M. S. Stockwell, H. Tang, H. van Bakel, V. Veguilla, R. Webby, D. C. Montefiori, D. J. Smith, Mapping SARS-CoV-2 antigenic relationships and serological responses. *Science* **382**, eadj0070 (2023).
42. S. H. Wilks, titertools. https://github.com/shwilks/titertools, (2023).
43. K. S. Corbett, S. M. Moin, H. M. Yassine, A. Cagigi, M. Kanekiyo, S. Boyoglu-Barnum, S. I. Myers, Y. Tsybovsky, A. K. Wheatley, C. A. Schramm, R. A. Gillespie, W. Shi, L. Wang, Y. Zhang, S. F. Andrews, M. G. Joyce, M. C. Crank, D. C. Douek, A. B. McDermott, J. R. Mascola, B. S. Graham, J. C. Boyington, Design of Nanoparticulate Group 2 Influenza Virus Hemagglutinin Stem Antigens That Activate Unmutated Ancestor B Cell Receptors of Broadly Neutralizing Antibody Lineages. *mBio* **10**, (2019).
44. H. M. Yassine, J. C. Boyington, P. M. McTamney, C. J. Wei, M. Kanekiyo, W. P. Kong, J. R. Gallagher, L. Wang, Y. Zhang, M. G. Joyce, D. Lingwood, S. M. Moin, H. Andersen, Y. Okuno, S. S.

Rao, A. K. Harris, P. D. Kwong, J. R. Mascola, G. J. Nabel, B. S. Graham, Hemagglutinin-stem nanoparticles generate heterosubtypic influenza protection. *Nat Med* **21**, 1065-1070 (2015).
45. H. X. Tan, S. Jegaskanda, J. A. Juno, R. Esterbauer, J. Wong, H. G. Kelly, Y. Liu, D. Tilmanis, A. C. Hurt, J. W. Yewdell, S. J. Kent, A. K. Wheatley, Subdominance and poor intrinsic immunogenicity limit humoral immunity targeting influenza HA stem. *J Clin Invest* **129**, 850-862 (2019).
46. World Health Organization, Serological diagnosis of influenza by microneutralization assay. *https://cdn.who.int/media/docs/default-source/influenza/2010_12_06_serological_diagnosis_of_influenza_by_microneutralization_assay.pdf?sfvrsn=b284682b_1*, (2010).
47. World Health Organization, WHO global influenza surveillance network: manual for the laboratory diagnosis and virological surveillance of influenza. *https://www.who.int/publications/i/item/manual-for-the-laboratory-diagnosis-and-virological-surveillance-of-influenza*, (2011).
48. W. Zhang, L. C. Rowntree, R. Muttucumaru, T. Damelang, M. Aban, A. C. Hurt, M. Auladell, R. Esterbauer, B. Wines, M. Hogarth, S. J. Turner, A. K. Wheatley, S. J. Kent, S. Patil, S. Avery, O. Morrissey, A. W. Chung, M. Koutsakos, T. H. Nguyen, A. C. Cheng, T. C. Kotsimbos, K. Kedzierska, Robust immunity to influenza vaccination in haematopoietic stem cell transplant recipients following reconstitution of humoral and adaptive immunity. *Clin Transl Immunology* **12**, e1456 (2023).
49. E. Lopez, E. R. Haycroft, A. Adair, F. L. Mordant, M. T. O'Neill, P. Pymm, S. J. Redmond, W. S. Lee, N. A. Gherardin, A. K. Wheatley, J. A. Juno, K. J. Selva, S. K. Davis, S. L. Grimley, L. Harty, D. F. Purcell, K. Subbarao, D. I. Godfrey, S. J. Kent, W. H. Tham, A. W. Chung, Simultaneous evaluation of antibodies that inhibit SARS-CoV-2 variants via multiplex assay. *JCI Insight* **6**, (2021).
50. J. R. Habel, B. Y. Chua, L. Kedzierski, K. J. Selva, T. Damelang, E. R. Haycroft, T. H. Nguyen, H. F. Koay, S. Nicholson, H. A. McQuilten, X. Jia, L. F. Allen, L. Hensen, W. Zhang, C. E. van de Sandt, J. A. Neil, K. Pragastis, J. S. Lau, J. Jumarang, E. K. Allen, F. Amanant, F. Krammer, K. M. Wragg, J. A. Juno, A. K. Wheatley, H. X. Tan, G. Pell, S. Walker, J. Audsley, A. Reynaldi, I. Thevarajan, J. T. Denholm, K. Subbarao, M. P. Davenport, P. M. Hogarth, D. I. Godfrey, A. C. Cheng, S. Y. Tong, K. Bond, D. A. Williamson, J. H. McMahon, P. G. Thomas, P. S. Pannaraj, F. James, N. E. Holmes, O. C. Smibert, J. A. Trubiano, C. L. Gordon, A. W. Chung, C. L. Whitehead, S. J. Kent, M. Lappas, L. C. ROWNTREE, K. Kedzierska, Immune profiling of SARS-CoV-2 infection during pregnancy reveals NK cell and γδ T cell perturbations. *JCI Insight* **8**, (2023).

Acknowledgments: The 1994 cohort study was originally sponsored by CSL Limited. We thank all the participants who were involved in the study. We thank the Melbourne Cytometry Platform for their services.

Funding: This research was funded in whole or part by the National Health and Medical Research Council Investigator Grants (EL1-1194036 to T.H.O.N., EL1-2009711 to H-X.T., EL1-2026357 to L.C.R., L3-2016491 to S.J.K., EL2-2008092 A.W.C., L1-2026762 to A.K.W. and L2-2033783 to K.K.); an Australian Research Council (ARC) Future Fellowship (FT200100928 to M.R.M.) and an ARC Discovery Project (DP230102850 to M.R.M.). The WHO Collaborating Centre for Reference and Research on Influenza is funded by the Australian Government Department of Health and Aged Care. For the purposes of open access, the author has applied a CC BY public copyright licence to any Author Accepted Manuscript version arising from this submission.

Author Contributions:

K.K. led the study. K.K., T.H.O.N., A.W.C. and A.K.W. supervised the study. T.H.O.N., I.J.H.F., R.A.P., H-X.T., W.Z., H.H.H., L.C.R., L.K., K.L., A.F., A.W.C., A.K.W. and K.K. designed the experiments. T.H.O.N., I.J.H.F., H-X.T., H.H.H. and L.F.A. performed and analyzed B cell probe experiments. R.R.H. analyzed B cell probe experiments. L.C. and A.J.H. performed antibody landscape and MN experiments. R.A.P. performed and analyzed multiplex experiments. T.H.O.N., I.J.H.F., S.H.W., M.R.M. and A.F. analyzed antibody landscape and MN data. L.C.A., H.A.M. and A.W.C. also analyzed multiplex data. H-X.T., S.J.K., K.L., S.R., A.F., A.W.C. and A.K.W. provided crucial reagents. G.A.T. established the 1994 cohort, and L.E.B. and G.D. prepared and cryopreserved the PBMC. S.R. provided archived cohort data. T.H.O.N., I.J.H.F., R.A.P., A.W.C., A.K.W. and K.K. wrote the manuscript. All authors reviewed and approved the manuscript.

Competing interests: K.K. received paid honoraria from Pfizer. K.L. and S.R. are employees of CSL Seqirus Ltd that manufacturers influenza vaccines and hold shares in the company. H.A.M. is a consultant for Ena Respiratory Pty. Ltd. All other authors declare no competing interests.

Data availability: All data associated with this study are in the paper or the supplementary materials. All materials used or generated in this study are commercially available or will be supplied upon reasonable request.

Figures legends

Fig. 1. 1994 IIV induces vaccine responses. (**A**) 1994 IIV cohort sampling timepoints and numbers for each assay. (**B** and **C**) Distribution of participants by sex (B) and age (C). (**D**) Exposure history of past and future circulating influenza virus strains. (**E**) HAI antibody titers towards 1994 IIV strains in subset of young and older adults from HAI landscape cohort. (**F**) Fold change in HAI responses from the HAI landscape cohort (d28/BL), where seroconversion is defined as 4 or more-fold change. For (C), (E) and (F), median and IQR are shown. Statistical significance was determined by Wilcoxon test for timepoint comparisons within an age group or Mann-Whitney for comparisons between younger and older adults. (**G**) Endpoint titers of HA stem-specific antibody responses to H1 and H3. Bar indicates mean for d28 timepoint. *P < 0.05, **P < 0.01, ***P < 0.001, ****P < 0.0001. (A to D) Data are from n = 89 young and n = 68 older adults. (E to G) Data are from n = 28 young and n = 28 older adults.

Fig. 2. 1994 IIV induces antibody titers against future H1N1 and IBV strains. (**A**) Phylogenetic tree of selected IAV and IBV reference strains. Red indicates 1994 IIV strains, black represent those selected for HAI testing on selected cohorts of n = 28 young and n = 28 older adults. (**B to G**) HAI titers were determined for H1N1 (B and C), H3N2 (D and E), and IBV (F and G). Heatmaps of HAI antibody responses are shown for each individual against H1N1 (B), H3N2 (D), and IBV (F) strains. Asterisks alongside age of younger adults indicate previously vaccinated with influenza vaccine. Vaccination history for older adults was not collected. Representative HAI antibody graphs of H1N1 (C), H3N2 (E), and IBV (G) strains. Median and IQR are shown. Statistical significance was determined by Wilcoxon test for timepoint comparisons within an age group or by Mann-Whitney for comparisons between adults and older adults. *P < 0.05, **P < 0.01, ***P < 0.001, ****P < 0.0001. (B-G) Data are from n = 28 young and n = 28 older adults.

Fig. 3. Vaccine-induced neutralizing antibodies were observed for H1N1 and IBV strains. (**A**) Microneutralization assay showing neutralizing antibodies against vaccine strains (A/Texas/36/1991 and B/Panama/45/1990) and future strains (A/California/7/2009 and B/Brisbane/60/2008). Median and IQR are shown. Statistical significance was determined by Wilcoxon test for timepoint comparisons within an age group. **P < 0.01, ***P < 0.001, ****P < 0.0001. (**B**) GMT landscapes split by age group and virus subtype. In each plot, the dashed gray line and open points show pre-vaccination GMTs for each isolate tested, whereas

the solid black line and solid points show post-vaccination GMTs. Areas shaded red show an increase in GMT from pre-post-vaccination, beige shows a decrease, and gray shows the level of background reactivity found in both pre- and post-vaccination samples. Dashed vertical black lines mark the vaccine strain for each subtype. Viruses are ordered by date of isolation on x-axis, giving an approximate genetic/antigenic progression. Viruses in bold indicate vaccine strain. (**A** and **B**) Data are from n = 28 young and n = 28 older adults.

Fig. 4. Multidimensional systems serology reveals antibody responses to vaccine and future viral strains. (**A to D**) Volcano plots of antigen-antibody features between timepoints for younger (A) and older (B) adults and between young and older adults at (C) baseline and (D) d28. Z-score differences in $\log_{10}$(MFI+1) for each variable from baseline to d28 post-vaccination were determined by Wilcoxon matched-pairs signed rank test, and between age cohorts by Mann-Whitney U test. P values were adjusted by Holm correction for multiple comparisons; unadjusted -$\log_{10}$ P values are plotted, with the horizontal threshold line plotted at an adjusted (-$\log_{10}$) P value of 0.05. (**E and F**) PCA plots of feature selected data from the dataset including 1994 vaccine antigens plus age as variable features comparing scores (E) and features (F) of antibody responses for young and older adults at baseline. 1994 vaccine antigens included H1-HA A/Texas/36/1991 and H3-HA A/Beijing/32/1992. (**G and H**) PCA plots of feature selected data from the dataset including post 1994 vaccine antigens plus age as variable features comparing scores (G) and features (H) of antibody responses for young and older adults at baseline. (A to H) Data are from n = 35 young and n = 35 older adults.

Fig. 5. 1994 IIV-boosted cross-reactive influenza-specific B cell memory responses. (**A**) Viability of 30-year cryopreserved PBMC samples. (**B**) Representative HA-probe staining for 1994 IIV strain-specific memory B cells. (**C**) Frequency of 1994 IIV strain-specific IgD^- B cells at baseline and d28 post-vaccination in younger adults (n_{H1N1} = 27, n_{H3N2} = 39 and n_B = 30) and older adults (n_{H1N1} = 26, n_{H3N2} = 39 and n_B = 30). (**D and E**) Representative staining (D) and frequency (E) of cross-reactive H1-specific B cell responses (n_{young} = 19, n_{older} = 18). (**F and G**) Representative staining (F) and frequency (G) of cross-reactive B/Yamagata-specific B cell responses (n_{young} = 30, n_{older} = 30). (**H to J**) Representative staining (H) and frequency of H5-specific, H7-specific (I) and cross-reactive H1/H5-specific (J) B cell responses (n_{young} = 10, n_{older} = 10). Medians and IQRs are shown for all quantification. Open circles depict <5 events. n are displayed in the figure. Statistical significance was determined by Wilcoxon test for timepoint comparisons within an age group or by Mann-Whitney for

comparisons between adults and older adults. *P<0.05, **P<0.01, ***P<0.001, ****P<0.0001.

Fig. 6. 1994 IIV-strain specific and cross-reactive memory B cell responses are activated following IIV. (**A and B**) Phenotypic (A) and isotypic (B) gating of total $CD19^+$ B cells and HA^+ IgD^- B cells (n_{young} = 56, n_{older} = 55). Graphs show the proportion of each phenotype and isotype among total B cells. **(C to J)** Phenotype (C, D, G, and I) and isotype (E, F, H, and J) distribution of 1994 IIV strain-specific memory B cells (C and E), cross-reactive H1 and IBV memory B cells (D and F), H5- and H7-specific memory B cells (G and H), and H1/H5 cross-reactive memory B cells (I and J). Only 5 events or more were analyzed for HA^+ IgD^- B cells. Samples with less than 5 events were intentionally excluded for more accurate analyses of phenotype and isotype data. *n* are displayed in the figure. Mean and SD are shown. Statistical significance was determined by ANOVA with Tukey's multiple comparisons test. *P<0.05, **P<0.01, ***P<0.001, ****P<0.0001.

Fig. 7. Correlations observed between HAI antibody titers, microneutralizing antibody titers, systems serology data, and B cell responses across young and older adults post 1994 IIV. (A to C) Correlation matrices showing Spearman correlation of HAI titers (n = 28 young and n = 28 older adults), microneutralization (MN) titers (n = 27 young and n = 28 older adults), isotype and Fc binding (n = 35 young and n = 35 older adults), and frequency of post-vaccination HA-specific B cell responses against vaccine strains A/Texas/36/1991 (n = 56 young and n = 52 older adults) (A), A/Beijing/32/1992 (n = 59 young and n = 48 older adults) (B), and B/Panama/45/1990 (n = 45 young and n = 40 older adults) (C). HAI and microneutralization titers were $\log_2$ transformed, and systems serology MFI values were $\log_{10}$ transformed. Spearman's rank correlation with P-values adjusted for false discovery rate (FDR) < 0.05 are shown.

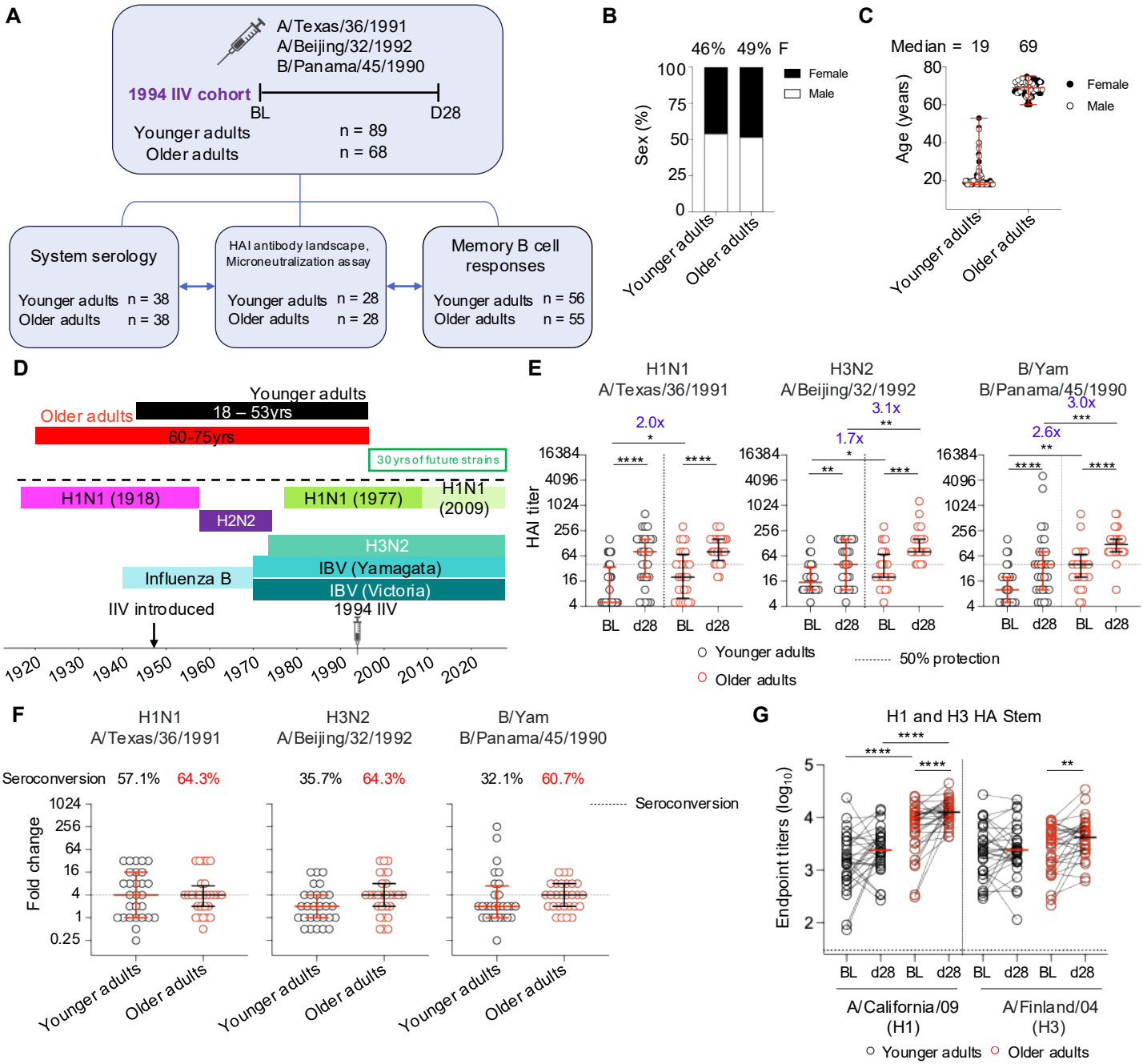

Nguyen et al. Figure 1

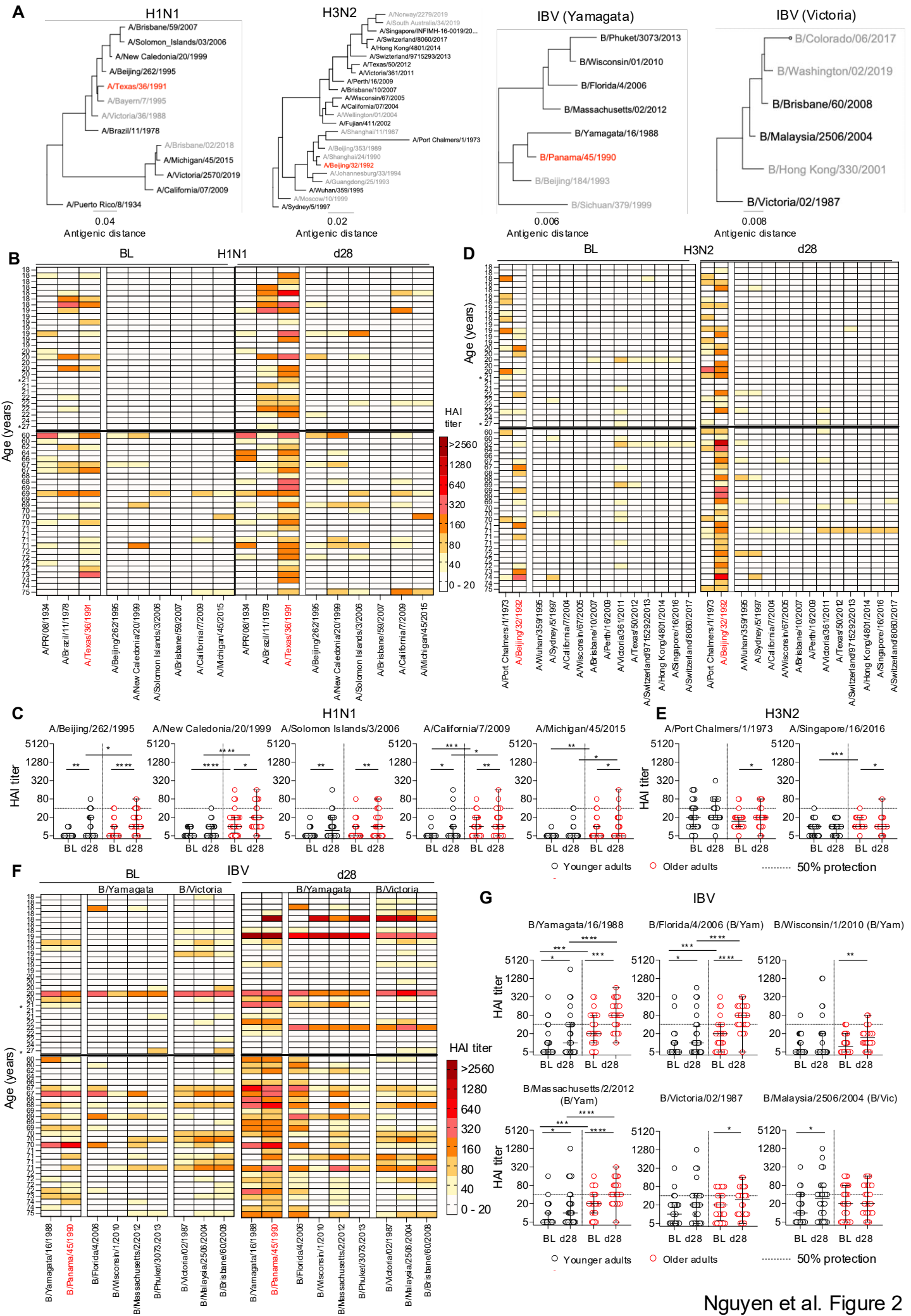

Nguyen et al. Figure 2

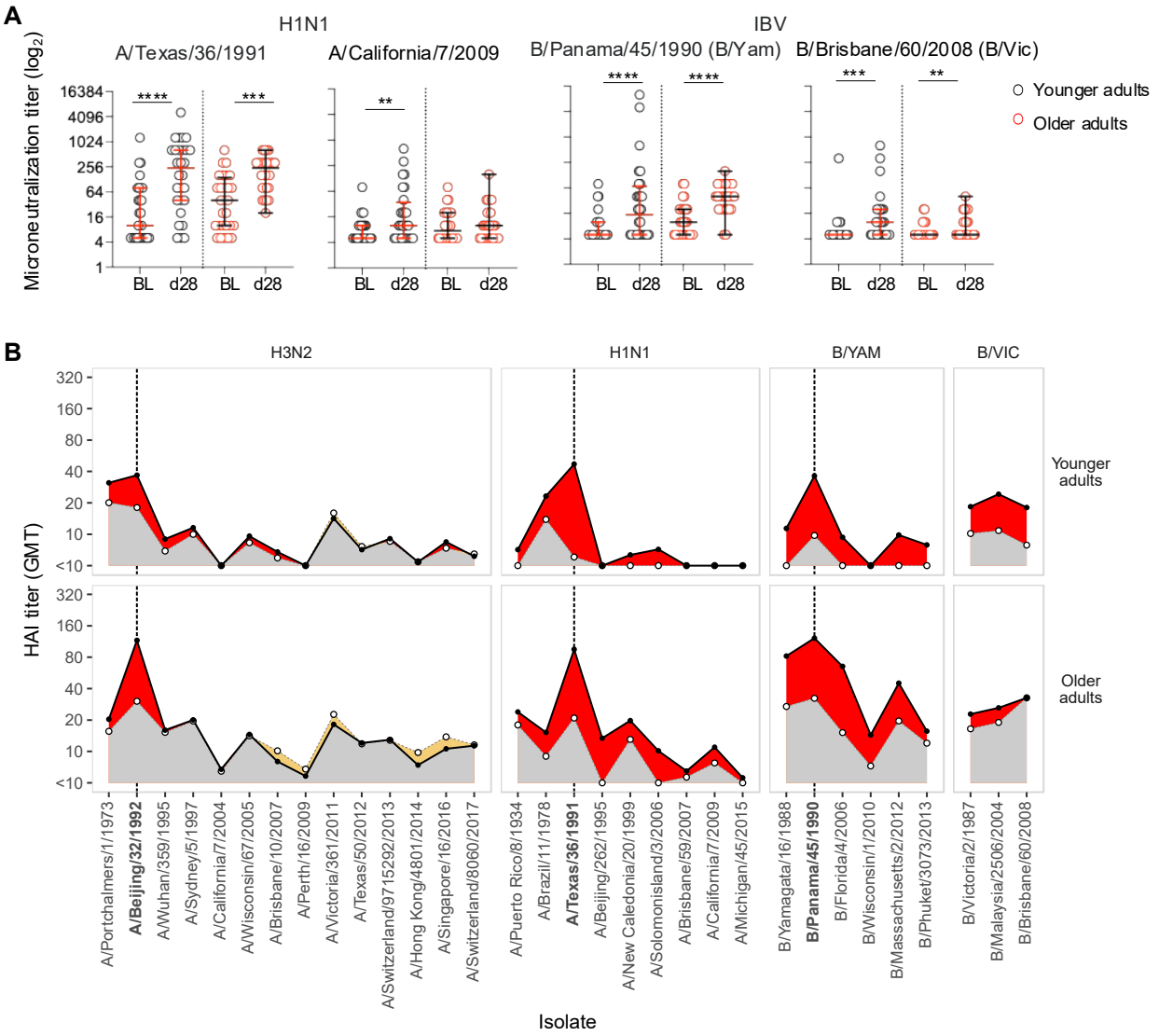

Nguyen et al. Figure 3

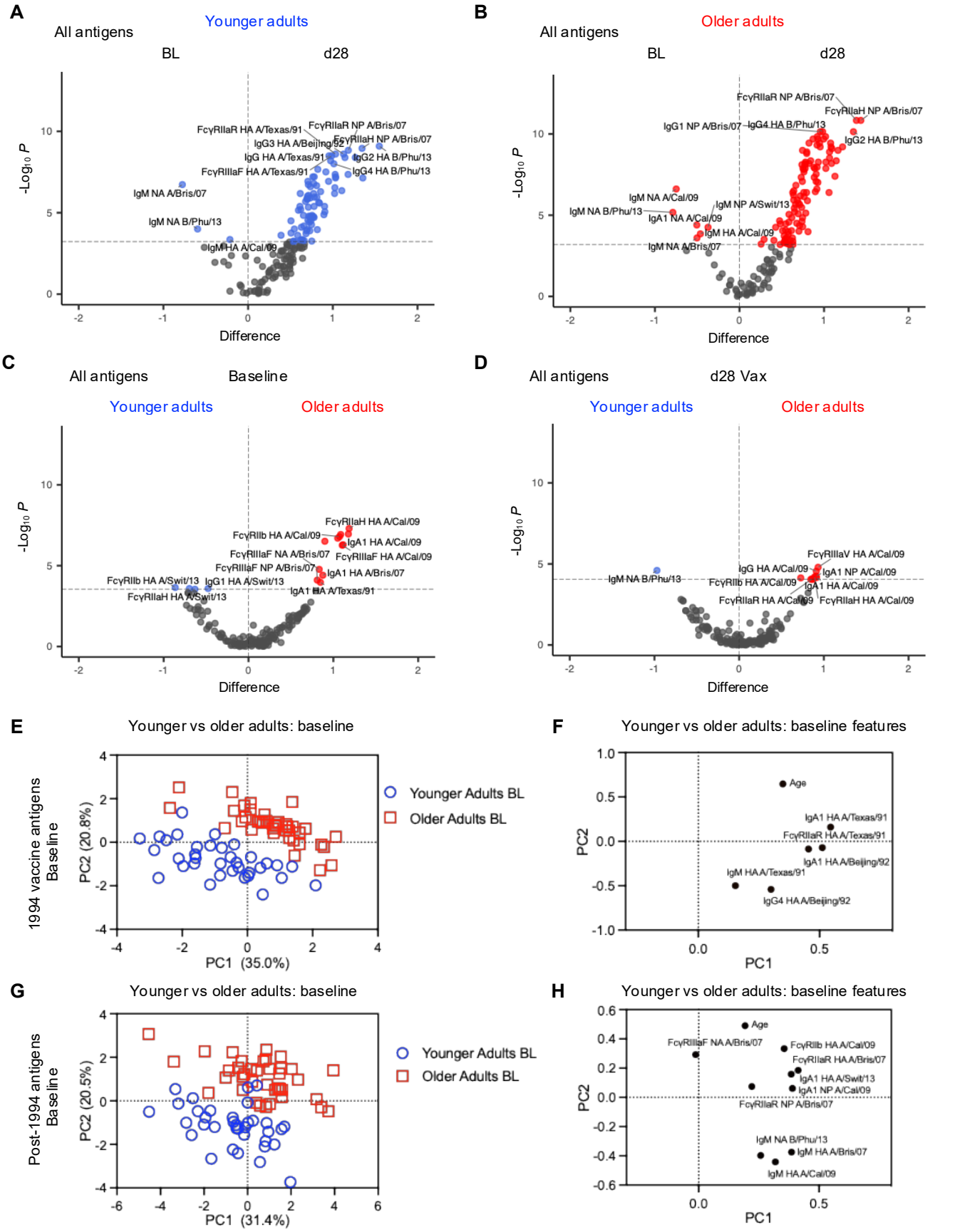

Nguyen et al. Figure 4

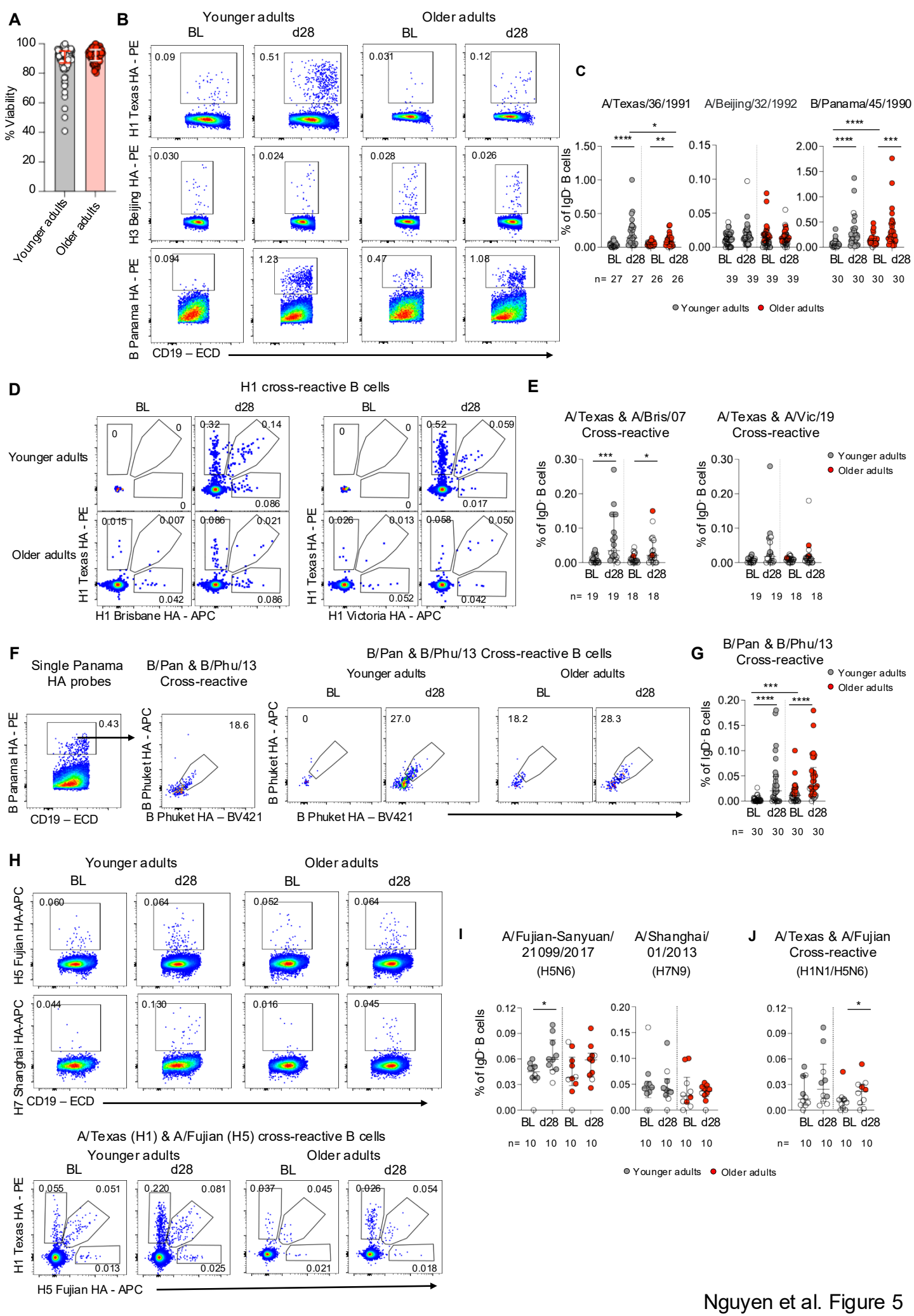

Nguyen et al. Figure 5

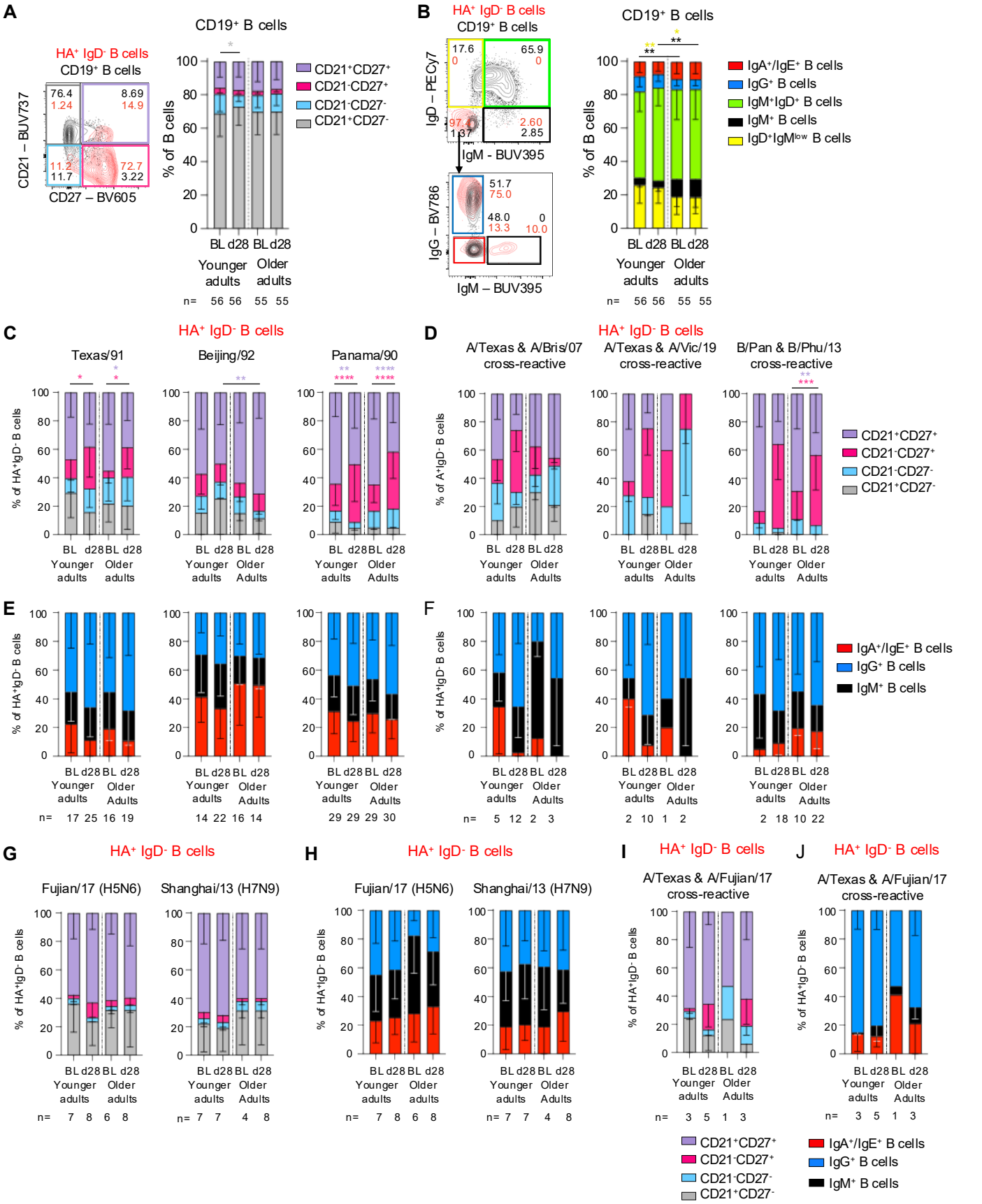

Nguyen et al. Figure 6

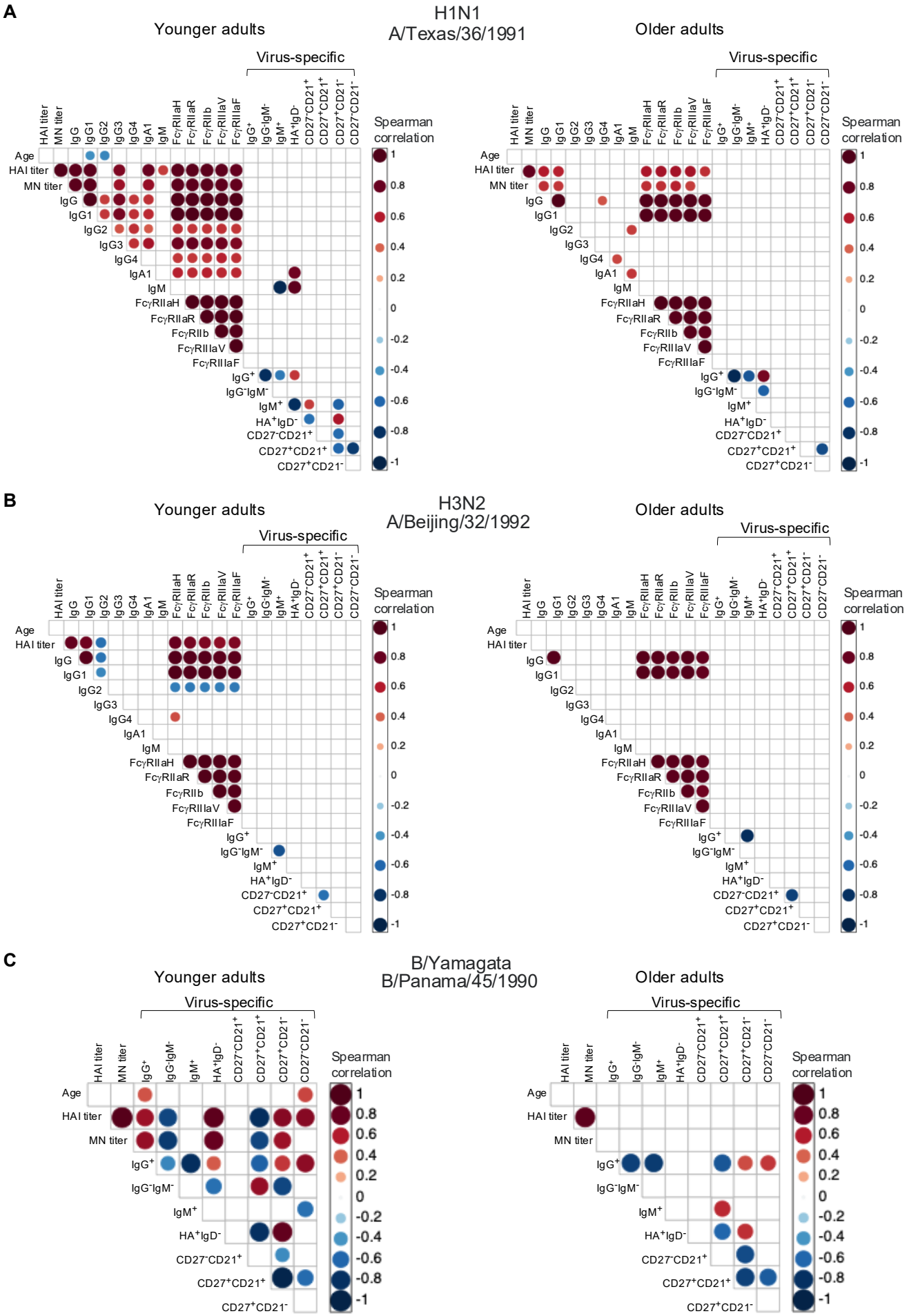

Nguyen et al. Figure 7